AD-A173 890 FIDELITY COHERENCE AND NOISE OF OCEAN BOTTOM SEISMOGRAPHS AND HYDROPHONES(U) RONDOUT ASSOCIATES INC STONE RIDGE NY G H SUTTON ET AL. 31 OCT 86 1/1

UNCLASSIFIED N00014-83-C-0009 F/G 8/11 NL

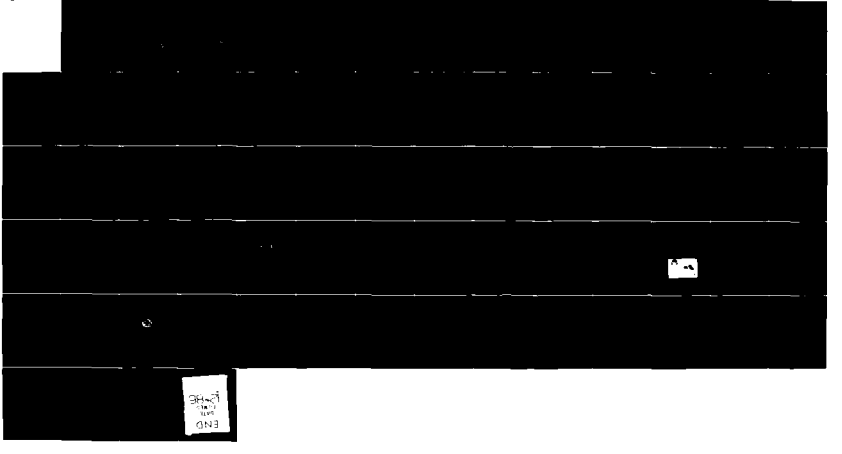

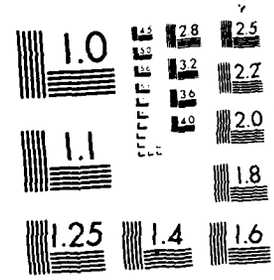

(12)

Final Report
to the
Office of Naval Research
for
Contract No. 00014-83-C-0009

FIDELITY, COHERENCE, AND NOISE OF OCEAN BOTTOM SEISMOGRAPHS AND HYDROPHONES

31
~~27~~ October 1986

Rondout Associates, Incorporated
P.O. Box 224
Stone Ridge, NY 12484

Final Report
to the
Office of Naval Research
for
Contract No. 00014-83-C-0009

FIDELITY, COHERENCE, AND NOISE OF OCEAN BOTTOM SEISMOGRAPHS AND HYDROPHONES

31 October 1986

Rondout Associates, Incorporated
P.O. Box 224
Stone Ridge, NY 12484

INTRODUCTION

The original purpose of this research was to investigate three outstanding problems associated with the use of ocean bottom seismographs and hydrophones:

1. mechanical coupling between an OBS and the ocean floor for both horizontal and vertical motion;
2. hydrodynamic coupling between an OBS and the near bottom water, both at seismic amplitudes and frequencies and at those associated with near bottom currents;
3. the relative advantages and disadvantages of seismometers versus hydrophones, singly or in arrays, for various hydroacoustic and seismic observations.

Because of a reduced funding level the third problem was not studied in detail.

The problem of coupling an OBS to soft, ocean bottom sediments has been of concern for some time. Recognizing this problem, ONR sponsored the Lopez Island OBS intercomparison experiment (Sutton et al, 1980 and 1981a). This experiment produced a great deal of quantitative information and provided a considerable amount of insight on directions to go for improving design. Taking advantage of knowledge gained at Lopez Island, two follow-up OBS coupling tests were conducted by personnel of Hawaii Institute of Geophysics in cooperation with RAI in Keehi Lagoon, Oahu in (Duennebier et al, 1981, Sutton et al, 1981b, Tuthill et al, 1981). In these tests, six different HIG operational and developmental OBS configurations were compared using calibrated mechanical transients, sine wave and white noise drivers, and explosions. A large amount of excellent data was generated during the Keehi Lagoon tests. We helped complete the analyses of this data and prepare the results for publication, emphasizing the quantitative aspects of the mechanical coupling tests and the amount of distortion expected for different OBS configurations.

The least understood, or studied, aspect of OBS coupling is the effect of the near bottom water, both in production of noise by interaction of currents and in signal distortion through seismic/hydroacoustic forces applied directly to the body of an OBS. Definite differences of "opinion" regarding the importance of water coupling became evident during and subsequent to the Lopez Island experiment. We have developed an appropriate theory and compared it with OBS data available at HIG in order to obtain a reliable estimate of the importance of water coupling as a function of OBS configuration. Laboratory tests employing a mass suspended in water on a shaker table confirmed theoretical predictions.

The paper "Optimum Design of Ocean Bottom Seismometers" by G. H. Sutton and F. K. Duennebier, which is submitted to Marine Geophysical Researches, summarizes the results of this research. An invited paper "Ocean Bottom Seismology: History and Current Status" by G. H. Sutton, presented at the SACLANT Ocean Seismo-Acoustics Symposium in June 1985 and published in the Proceeding volume (1986, T. Akal and J. M. Berkson, eds.) includes some of these results and a summary of the current status of OBS technology. Both of these papers are included in this Final Report. "A Comment on 'the Recovery of True Particle Motion from Three-Componet Ocean Bottom

Seismometer Data' by J. D. Garmany" by G. H. Sutton, F. K. Duennebier, and G. J. Fryer is also included in this report. The shaker table used in the laboratory tests was described in a paper by F. K. Duennebier, G. H. Sutton, D. Harris, and D. Byrne, "A Simple Shaker Table for Seismometer Calibration", Marine Geophysical Research, 6, P. 311-328, 1984.

REFERENCES

Duennebier, F. K., J. D. Tuthill, and G. H. Sutton, "Keehi OBS coupling test," *EOS (Abstract)*, vol. 62, p. 952, 1981.

Sutton, G. H., B. T. R. Lewis, J. Ewing, F. K. Duennebier, B. Iwatake, and J. D. Tuthill et al., "Lopez Island ocean bottom seismometer intercomparison experiment final report to ONR," *HIG*, vol. 80-4, 272 pp, 1980.

Sutton, G. H., F. K. Duennebier, B. Iwatake, J. D. Tuthill, B. T. R. Lewis, and J. Ewing, "An overview and general results of the Lopex Island OBS experiment," *Marine Geophys. Res.*, vol. 5, pp. 3-34, 1981a.

Sutton, G. H., F. K. Duennebier, and J. D. Tuthill, "Mechanical transient tests of OBS-bottom coupling," *EOS (Abstract)*, vol. 62, p. 953, 1981b.

Tuthill, J. D., F. K. Duennebier, and G. H. Sutton, "Sediment structure and acoustic properties in Keehi Lagoon, Oahu," *EOS (Abstract)*, vol. 62, p. 953, 1981.

OPTIMUM DESIGN OF OCEAN BOTTOM SEISMOMETERS

George H. Sutton
Rondout Associates, Inc.
P.O. Box 224, Stone Ridge, New York 12484

Frederick K. Duennebier
Hawaii Institute of Geophysics, University of Hawaii
2525 Correa Road, Honolulu, Hawaii 96822

October 28, 1986

Abstract

Ocean bottom seismometers (OBS) have been widely used during the past decade to collect seismic data for determination of the structure of the oceanic lithosphere, stress patterns in regions of earthquake activity, and geo-acoustic parameters of the ocean floor. Data quality from these experiments has often been disappointing because of poor signal quality and high noise levels. Many of these problems result from motion of the OBS package that is decoupled from motion of the ocean floor. These coupling problems are more serious in the ocean than on land because of the low shear strengths of most ocean sediments. In this paper we continue to develop the theory of coupling of OBSs to soft sediments and arrive at results suggesting that OBS packages should be designed with: (1) the minimum mass possible, (2) radius of area in contact with the sediment proportional to the cube root of the mass, and the maximum radius less than 1/4 of the shear wavelength, (3) density of the OBS approximately that of the sediment, (4) a low profile and a small vertical cross section with the water, and (5) low density gradients, and maximum symmetry about the vertical axis. Agreement of the theory with test data is good; most deviations are reasonable, given limitations of the theory and experiments. The theory also suggests that the coupling frequency, the frequency above which the OBS does not follow the motion of the sediment, is directly proportional to the sediment shear velocity.

1 INTRODUCTION

Seismometers are instruments designed to measure the motion of the material they are attached to. A well-designed seismometer will detect this motion with high fidelity and low noise over a broad range of amplitudes and frequencies, modifying the motion only by a known transfer function. These characteristics are relatively easy to achieve on land by careful placement of seismometers in low noise environments on materials with high shear strengths. [Krohn (1984)]

discusses problems associated with coupling of exploration geophones to different soils for frequencies above 100 Hz. There are few locations on the ocean bottom with high shear strengths, and finding a low noise site is a matter of chance. High-quality data can be obtained from the ocean bottom by: (1) avoiding experiments in soft sediments, (2) using only hydrophones, which are much less sensitive to coupling problems than seismometers but can not directly detect shear arrivals [Koelsch and Purdy (1979)], (3) avoiding the low-shear sediments entirely by emplacing seismometers in boreholes, which is very expensive [Duennebier et.al. (1981),Byrne et.al. (1983)], (4) trying to determine the change in the transfer function caused by coupling problems [Zelikovitz and Prothero (1981)], or (5) designing OBSs that will not be sensitive to coupling problems. Although several attempts have been made to design OBSs to minimize coupling problems [Duschenes et.al. (1981),Trehu and Solomon (1981),Byrne et.al. (1983)], the attempts have suffered from the lack of a coupling theory that defines the parameters that are critical to OBS design.

In this paper we present theoretical arguments that define the parameters important to design of OBSs. Results are compared with data obtained from the Lopez Island OBS Intercomparison Experiment [Sutton et.al. (1981b)], two experiments conducted in Keehi Lagoon, Oahu, and laboratory experiments on a shaker table. Two theories are presented to explain the motions of OBSs on soft sediments, one (the spring-mass theory) is appropriate for low frequencies and sediments that are treated as an elastic solid, but it is difficult to extrapolate this theory to high frequencies. The other theory (the fluid theory) is appropriate at high frequencies and when the sediment can be treated as a fluid. These theories agree well with each other except for one term, the amount of sediment entrained in the motion of the OBS.

The spring-mass theory was originally developed by structural engineers to analyze the vibrations of foundations. It has been used by seismologists to model the behavior of seismometers in swamps, and was applied to the OBS case by including buoyancy [Sutton et.al. (1981a)]. In the previous paper, we had no theoretical basis to determine how much water and sediment are in-

cluded in the motion of the OBS when it moves relative to the sediment. In this paper, the theory is developed to include the entrained water and sediment. The fluid theory is a result of studies of the motions of bodies immersed in fluids [Bachelor (1967)]. The motions of spheres and disks in fluids is studied to obtain equations for the motions of OBSs in fluids. The resulting formulations are compared with experimental field data for coupling of vertical motion, and with laboratory data for both vertical and horizontal motion. Each theory is valid when used to predict the motion of OBSs in different situations. The theories agree well with the data, and clearly imply guidelines for design of OBSs for optimum coupling to the bottom, despite problems of not understanding the motions in all cases. In addition to the design constraints implied by the theory, other design constraints, such as small cross section in the water and symmetry about the vertical axis, are also discussed to show ways of minimizing cross coupling and coupling of water motion to motion of the OBS.

2 THEORY

2.1 Spring-Mass Theory

A seismograph sitting on a compliant ocean floor has six degrees of freedom of motion: translation and rotation in the vertical and two orthogonal directions. For our purposes, we shall ignore rotation about the vertical axis, and concentrate on translation in the vertical direction. Each degree of freedom can support a mode of oscillation with a characteristic frequency and damping. In general, the modes will be coupled. For a well-designed instrument, however, only horizontal translation and rocking about the orthogonal horizontal axis may be strongly coupled. Radial symmetry about the vertical axis, which does not exist, for example, with the commonly used tripod support, is required for horizontal coupled modes to be independent of azimuth. The vertical modes are decoupled with a good tripod mount.

Forces impinge on the OBS from both the sediment and the water. Differential horizontal motion across the water-sediment boundary, both from seismic waves and from bottom currents,

can produce distortion, cross coupling, and noise.

Much of the theory required for the analysis of dynamic coupling between an OBS and the bottom has been developed by structural engineers for the design of foundations resting on soils. [Hsieh (1962)] provided a clear summary of this work along with references to important earlier work. [Safar (1978)] applied the theory to investigate the minimization of distortion caused by coupling between the ground and vertical geophones. (He uses the dynamical interaction between a number of geophones to improve the transient response to seismic signals.) These studies do not include the effects of the water. [Sutton et.al. (1981a)], [Sutton et.al. (1981b)], [Zelikovitz and Prothero (1981)], and [Trehu (1985a)] consider the coupling and seismic response of an OBS surrounded by water. This paper is an extension of that work.

First, we review the equations appropriate for the motion of an instrument on a uniform elastic half-space in the absence of water, and then include the effect of the water. Only vertical motion will be considered in detail. Horizontal coupling and the effect of layering or gradients within the bottom will be considered briefly.

The detailed analysis of the dynamic response of a rigid body resting on a solid half-space is quite complex. In general, the frequency response depends upon the instrument mass, and the size, shape, and stress distribution of the contact area, and the shear velocity, density, dissipation, and Poisson's ratio versus depth in the half-space. [Hsieh (1962)] provides equations appropriate for a rigid circular disk on a homogeneous, isotropic elastic medium for vertical and horizontal translation and for rotation about vertical and horizontal axes. The coefficients of the solutions depend upon Poisson's ratio and the ratio of the contact radius to the wavelength of shear waves in the medium. These coefficients can be modified for different shapes and distributions of contact pressure. [Safar (1978)] summarized equivalent results for vertical motion only. [Luco (1974)] calculated impedance functions for rigid foundations on a layered medium and concluded that, in contrast with a uniform half-space, a layered medium shows stronger frequency dependence and reduced radiation damping (higher Q resonances) at low frequencies.

Typical ocean bottom sediment can have a shear velocity, v_s, less than 50 m/s and, perhaps, as low as 10 m/s; compressional velocity, v_p, is near that for water, 1.5 km/s; and density, ρ_s, ranges between about 1300 and 1800 kg/m^3. Thus, for the relations used in this paper, we shall assume Poisson's ratio, $\sigma = 0.5$ (nearly fluid) and $\rho = 1570\ kg/m^3$. The equations presented are appropriate only for shear wavelengths, λ_s, greater than 4 times the bearing radius, r. This can be a serious restriction since, for example, at $v_s = 20\ m/s$ and 20 Hz, the radius should be less than 0.25 m.

The response of the seismograph frame, I, to a vertical seismic input signal, Z, in the absence of water and assuming a negligible mass of sediment is displaced by the instrument is given by [Safar (1978)] as

$$I/Z = [(\omega_c S/Q) + {\omega_c}^2]/[S^2 + (\omega_c S/Q) + {\omega_c}^2] \tag{1}$$

where $\omega_c = [K(a)/M_i]^{1/2}$ = coupling frequency (2)

$$Q = [K(a)M_i]^{1/2}/R(a) \text{ = quality factor} \tag{3}$$

M_i = OBS mass

and S = the Laplace transform variable.

The dynamical spring constant, K, and the damping coefficient, R, are both functions of the dimensionless frequency given by,

$$a = \omega r/v_s = 2\pi r/\lambda_s$$

and, therefore, ω_c and Q in equation 1 are also functions of frequency.

For a circular disk on an elastic half space,

$$K = v_s^2 \rho_s r F_1(a) \text{ and } R = v_s \rho_s r^2 F_2(a)/a. \tag{4}$$

For $\sigma = 0.5$ and $0 \leq a \leq 1.5$,

$$F_1 \simeq 8.0 - 2.0a^2 \text{ and } F_2 \simeq 6.9a \text{ [Hsieh (1962)]}. \tag{5}$$

F_1 and F_2 have different values for different shaped OBSs, and for horizontal translation or rotation about horizontal or vertical axes.

In Figure 1, the approximate values for F_1 and F_2 given by equations 5 are shown to agree well with values obtained from detailed calculations by Bycroft [Bycroft (1956),Arnold et.al. (1955)]. *FIG 1*

Substituting equations 4 and 5 in equations 2 and 3 and solving for $\omega = \omega_c$ we obtain

$$\omega_c = [K_0/M']^{1/2} \tag{6}$$

and

$$Q = 1/2h = a_c b/6.9 = 0.41b/(b+2)^{1/2} \tag{7}$$

where $K_0 = 8\rho_s v_s^2 r =$ static spring constant, $\sigma \simeq 0.5$ [Hsieh (1962)] (8)

$$M' = M_i + 2\rho_s r^3 = \text{ effective mass, instrument plus sediment} \tag{9}$$

$$a_c = \omega_c r/v_s = \text{ dimensionless resonant frequency} \tag{10}$$

$$b = M_i/\rho_s r^3 = \text{ dimensionless shape factor} \tag{11}$$

Some algebra also shows that $a_c^2 = 8/(b+2)$ and, since equation 5 is valid only for values of a less than about 1.5, this requires that $b \geq 1.56$, i.e., the instrument mass, $M_i \geq 1.56\rho_s r^3$. Figure 2 shows the increase of effective mass, M', and fraction of critical damping, h_c, with increase in dimensionless resonant frequency, a_c. *FIG 2*

Because of the dependence of K_0 and M' on r, for given (disk-shaped) instrument mass and sediment parameters, the coupling frequency exhibits a maximum value with increasing r. This can be seen in Figure 3, which is a plot of coupling frequency versus bearing radius for different values of instrument mass, M_i, from Equation 6, 8, and 9. Assuming that the maximum coupling frequency is desirable, the optimum radius and maximum coupling frequency, also obtained from Equations 6, 8, and 9 is: *FIG 3*

$$r_{opt} = (M_i/4\rho_s)^{1/3} \tag{12}$$

$$f_{c\ max} = 0.292 v_s (\rho_s/M_i)^{1/3}. \tag{13}$$

At the optimum coupling condition: $b = 4$, $a_c = 1.16$ and $Q = 0.67$. The increase in τ_{opt} and decrease in maximum coupling frequency, $f_{c\ max}$, with increasing instrument mass obtained from Equations 12 and 13, are shown in Figure 4. *FIG 4*

2.2 Fluid Theory

The above analysis does not include any effects of the water surrounding the OBS above the sediment. Before including this effect, and its complicated boundary conditions, we will study the motion of an OBS surrounded only by a fluid.

The water affects the seismic response of the instrument in two ways: 1) a buoyancy effect that reduces the effective force of the seismic signal on the instrument and depends upon the volume of water (and sediment) displaced; and, 2) an added virtual mass that depends upon the cross-sectional area and shape of the instrument. [Bachelor (1967)] gives the equation for the motion of a rigid sphere, v_i, in response to the motion of an acoustic wave in fluid, v_w, for wavelengths large compared to the diameter of the sphere:

$$v_i/v_w = 3/(2(M_i/M_w) + 1) \tag{14}$$

where M_i and M_w are the masses of the sphere and displaced water, respectively. Figure 5 is a plot of Equation 14 for M_i/M_w between 0 and 3. This indicates amplification approaching a factor of 3 for low sphere densities and attenuation for high densities. When the densities of the sphere and water are equal (neutral buoyancy) the motions are equal. Many operational OBSs have a large vertical gradient in density, with a dense lower support structure and buoyant superstructure. Based on the above analysis, horizontal signals are expected to produce strong torques in such instruments. *FIG 5*

The virtual mass M_v, for a sphere immersed in water is $M_w/2$; that for a cylinder is M_w; and that for a disk is $(8/3)\rho_w r^3$ [Bachelor (1967)]. The motion of a disk in water, when the relative motion is normal to the plane of the disk, is given by:

$$v_i/v_w = \frac{1 + 8r/3\pi t}{\rho_i/\rho_w + 8r/3\pi t} \tag{15}$$

where ρ_i and ρ_w are the disk and water densities, t is the disk thickness, and r is the disk radius. Equation 15 is plotted in Figure 6 showing v_i/v_w as a function of r/t for several values of ρ_i/ρ_w. *FIG 6* This motion is much different than that of a sphere in that the radius of the sphere has no effect on its motion, but the "flatness" of the disk is a very important parameter in its motion. This change in response with shape is related to the ease with which water can move past the body in the direction of motion. The flatter the disk, the more difficult it is for water to move past the disk, and the larger the mass of water (virtual mass) that moves with the disk. In the OBS case, one wants the OBS to move with the sediment, not with the water, thus a large virtual sediment mass (relative to M_i) and small virtual water mass are desired.

On a fluid-fluid boundary, we can approximate the motion of a disk between two fluids by simply dividing the virtual mass into two equal parts with the appropriate densities: $M_v = 4(\rho_s + \rho_w)r^3/3$. We have no rigorous basis for doing this, and this formula does not account for energy radiated away along the boundary. We expect, however, that this value of M_v is a good approximation for small motions. With this definition for virtual mass of a disk, the velocity of the disk relative to a fluid-fluid interface for motion perpendicular to the interface is :

$$\frac{I}{Z} = \frac{\frac{\rho_w}{(\rho_w+\rho_s)} + 4r/3\pi t}{\frac{\rho_i}{(\rho_w+\rho_s)} + 4r/3\pi t} \tag{16}$$

This equation is the same as Equation 15 if $\rho_w = \rho_s$.

Here we note that if $\rho_w = 0$, we should have the same result as for Equation 1 when $K_0 = 0$, or in the high frequency limit ($\omega \gg \omega_c$). This is not the case because Equation 1 approaches zero when $\omega \gg \omega_c$, and Equation 16 is a constant given by $(\frac{3\pi\rho_i t}{4\rho_s r} + 1)^{-1}$ when $\rho_w = 0$. When the spring constant is set to zero in Equation 1, $I/Z = [(M_i S/R) + 1]^{-1}$, which is a low pass filter function. While both equations are valid in their range of interest, they yield very different results in these cases. Looking more closely at the differences, the fluid theory includes no radiation of energy away from the body, while the spring-mass theory does. The increase in virtual mass generally observed near a boundary where flow is restricted is also not included [Milne-Thompson (1950)]. We expect that Equation 1 yields the correct results on an interface when $K_0 \neq 0$, and we now include the

effects of water above the interface in the equations.

2.3 Spring-Mass theory with water

Since the bottom sediments are "nearly" fluid, in this paper we shall use the fluid dynamic relations as a first approximation to the virtual mass of the water (in addition to the term, already included in Equation 9 for the sediment side of the boundary obtained from the dynamical spring constant). Note that the virtual mass is a function of shape, and it can change with the direction of motion.

The vertical component of the equation of motion for the instrument frame including the effect of water can be written in Laplace transform notation as

$$(M_i + M_v)S^2 I + RS(I - Z) + K(I - Z) = (M_w + M_s + M_v)S^2 Z \tag{17}$$

where M_w and M_s represent the mass of water and sediment, respectively, displaced by the instrument, and M_v is its virtual mass of water entrained in the motion. Note that for a sphere in the absence of sediment, i.e. $R = K = M_s = 0$ and $M_v = M_w/2$, Equation 17 reduces to Equation 14 that gives the response of a sphere to an acoustic wave in a fluid. From Equation 17 we can obtain an expression for the response of the OBS frame to a vertical seismic input, in the presence of water,

$$I/Z = \frac{\alpha(S^2 + \omega_c' S/\alpha Q' + \omega_c'^2/\alpha)}{(S^2 + \omega_c' S/Q' + \omega_c'^2)} \tag{18}$$

where

$$\alpha = (M_w + M_s + M_v)/M_i^* \tag{19}$$

and ω_c' and Q' are shape-dependent parameters, given by Equations 6 to 11 for disk-shaped OBS footpads, with the instrument mass, M_i, replaced by the dynamic mass:

$$M_i^* = (M_i + M_v).$$

Equation 18 is similar to that given by [Sutton et.al. (1981a)], with their coupling coefficient, C, replaced by $(1 - \alpha)$. However, the dynamic mass of sediment included in the earlier definition of C

is not represented in α. Sutton et al. defined $(1 - C)$, equivalent to our α, as

$$(1 - C) = \frac{M_w + M_s + M_v + M_s^*}{M_i^* + M_s^*} \tag{20}$$

where M_s^* represents the sediment that moves with the OBS. Comparing Equations 19 and 20, we see that $\alpha \leq (1 - C)$. Although an effective sediment mass ($2\rho_s r^3$, arising from the dynamical spring constant K, for a disk-shaped area in contact with the sediment) is included in the resonant frequency and damping terms through Equations 6 and 7, apparently it is not required as an additional virtual mass to that of the water, M_v. In the absence of water, $M_w = M_v = 0$, and with negligible displaced sediment, $M_s = 0$, α becomes zero and Equation 18 reduces to Equation 1. We note, however, that this equation does not yield the desired result (Equation 15) as the interface disappears when K approaches zero, and ρ_s approaches ρ_w for a disk-shaped OBS.

[Sutton et.al. (1981a)] added a buoyancy term to the restoring force supplied by the elasticity of the sediment:

$$K_T = K + (\rho_s - \rho_w)\pi r^2 g$$

where g is the acceleration of gravity. It is unlikely that the latter term will be important in practical situations, as shown below. The ratio of the first term (K) to the second is, using Equation 8 and taking $K_0 = K$,

$$\frac{K}{(\rho_s - \rho_w)\pi r^2 g} = \frac{8v_s^2\rho_s r}{10\pi r^2(\rho_s - \rho_w)}.$$

For a sediment with $v_s = 10m/s$ and $\rho_s = 1300\ kg/m^3$ this ratio has a value of $110/r$, thus K_T is not affected by buoyancy unless r is very large.

From Equation 18 we see that the response of the OBS frame to a seismic input signal can be defined with three parameters: ω_c'; Q'; and α. These, in turn, depend upon the shape and mass of the instrument package and the elastic properties of the bottom sediment. The transfer function is 1 for all frequencies when the coupling coefficient, α, equals 1 i.e., neutral buoyancy ($M_i = M_w + M_s$ in Equation 19) and no net dynamic force. By substituting $j\omega$ for S, the Laplace transform variable, in Equation 18, we can separate the real and imaginary parts, and obtain the

amplitude transfer function for seismic wave input $A = (real^2 + imaginary^2)^{1/2}$, and the phase response $\phi = tan^{-1}(imaginary/real)$. These are found to be:

$$A_S = \left[\frac{(\omega_c'^2 - \alpha\omega^2)^2 + 4h'^2\omega_c'^2\omega^2}{(\omega_c'^2 - \omega^2)^2 + 4h'^2\omega_c'^2\omega^2}\right]^{1/2} \tag{21}$$

and,

$$\phi_S = tan^{-1}\left[\frac{2h'(\alpha-1)\omega^3\omega_c'}{(\omega_c'^2 - \alpha\omega^2)(\omega_c'^2 - \omega^2) + 4h'^2\omega_c'^2\omega^2)}\right]. \tag{22}$$

Solutions to these equations for various values of α and h are shown in Figures 7 and 8. When *FIG 7 Fi*
$\omega = \omega_c'$, the amplitude and phase are given by:

$$A_S = \left[\frac{1 + (1-\alpha)^2}{4h'^2}\right]^{1/2}$$

and

$$\phi_S = tan^{-1}((\alpha - 1)/2h').$$

Note that the above equations and 18,19,21, and 22 do not depend explicitly on OBS shape.

The curves in Figures (7) and (8) are for the approximation that the coefficients Q' $(= 1/2h')$ and ω_c' are constant. When response curves using constant coefficients are compared with those obtained by using coefficients that vary with frequency according to Equations 4 and 5, the response is within 1 dB amplitude and 5° phase difference for $\omega < 1.5\omega_c'$. For this reason, we ignore the frequency variation of ω_c' and Q' in the remainder of this paper.

As indicated above, the parameters ω_c', Q', and α may be calculated using equations 6 to 11 with M_i replaced by M_i^* (for disk-shaped area in contact with the sediment) and Equation 19 for a particular instrument design and sediment, as M_v is strongly dependent on the shape of the OBS in the water. These parameters can also be determined experimentally from an in situ calibration, as discussed below.

2.4 Transient tests

A force can be applied to an OBS by the release of a float [Sutton, et,al., 1981a], or, alternatively, by use of an internal shaker [Zelikovitz and Prothero (1981)]. Such calibration transients have been

applied to both operational and prototype instruments. The motion of the OBS caused by a force, $\mathcal{F}$, on the OBS is given by the following equation:

$$I = \frac{\mathcal{F}}{[M_i^*(S^2 + \omega_c' S/Q' + \omega_c'^2)]} \tag{23}$$

Equation 23 can be obtained from equation 17 by replacing the right hand side by $\mathcal{F}$ and setting $Z = 0$. Using Equation 23 or its Laplace transform, the dynamic mass M_i^* and the coupling frequency, ω_c', and Q' can be obtained by matching the observed spectra or the time transients (after correcting for the response of the geophone) to theoretical response functions or their time equivalents, for a known calibration force, $\mathcal{F}$. The coupling coefficient, α, can be calculated using Equation 19. The use of Equation 23 should be valid independent of the exact nature of virtual mass, M_v, and whether or not the sediment contributes to that term. The amplitude and phase functions obtained from Equation 23 for a float transient test ($\mathcal{F} = F/S$) are given by:

$$A_T = \frac{F}{M_i^*} \left\{ \omega \left[(\omega_c'^2 - \omega^2)^2 + \omega_c'^2 \omega^2 / Q'^2 \right]^{1/2} \right\}^{-1} \tag{24}$$

and

$$\phi_T = tan^{-1} \left[\frac{\omega_c'^2 - \omega^2}{2h'\omega_c'\omega} \right]. \tag{25}$$

3 Experimental Data

3.1 Laboratory test

A Laboratory test was conducted using the shaker table facility at the Hawaii Institue of Geophysics[Duennebier et.al. (1984)] to verify the responses of a sphere to seismic waves predicted by equations 21 and 22. In this test a platform isolated from ground vibrations by a weak spring is excited with motion having a near-white spectrum in a vertical or horizontal direction. The motion is detected by a geophone rigidly mounted to the platform, and by an identical geophone mounted in a sphere suspended from the platform by a spring representing the sediment (Figure 9). The transfer function of the suspended geophone (T in the figure) relative to the reference geophone

FIG 9

(R) yields the coupling response, and should be predicted by Equations 21, and 22 within the experimental errors.

Two tests are discussed here, one for vertical motion using a buoyant sphere, and one for horizontal motion using a heavy sphere, both motions were measured with the spheres in air, and immersed in water. Data on the spheres and test results are given in Table 1. The low density *T 1* sphere was used in the vertical test to avoid problems of non-linearity in the suspension. By using a density of about $0.5gm/cm^3$, the spring extension in air, is the same as it is in water, although the spring is mounted on top of the sphere in air and on the bottom in water. The amplitude and phase results from the tests in air, digitized from the output of a spectrum analyser, are shown in Figure 10 together with suitable solutions of equations 21 and 22 with $\alpha = 0$. Note that the theory *FIG 10* and data are in excellent agreement.

When the spheres are immersed in water, two effects are expected: 1) the frequency of resonance should decrease because of the added virtual mass; and 2) at high frequencies the amplitude response should become constant and the phase response should return to zero because of the buoyancy effect. As seen in Figure 11, each of these effects is observed. For the vertical case, the change in α is *FIG 11* as predicted using the constants computed from Equation 19 and Table I within the experimental errors (the spectra were digitized from 3" by 4" photographs taken from the Spectrum Analyser). The changes observed in the horizontal test are as predicted except that the value of α predicted is about twice as large as that observed from the data, as shown by the frequency of the spectral low at about 11 Hz, and the lower than expected response at high frequencies. The reason for this discrepancy is not known, and is puzzling since the change in coupling frequency from air to water is very close to that predicted (8.3 Hz to 7.05 Hz). It is likely that this problem results from the finite size of the water tank and shallow water depth used to immerse the sphere. This failure is serious in that proper estimates of the value of α are vital in order to correct transfer functions obtained by internal calibration devices to the sesimic transfer function. It appears that α is sensitive to the geometry of the instrument and to the relationship to nearby interfaces. If α is not accurately

	Vertical Test	Horizontal Test
Sphere diameter, cm	12.7	10.2
Sphere volume, cm^3	1070	549
Sphere mass, gm	454	850
Sphere density, gm/cm^3	0.424	1.55
Mass displaced water, gm	1070	549
Dynamic mass, $(M_s + M_v)$, gm	989	1125
Coupling frequency, Hz, observed in air	7.2	8.6
Coupling frequency, Hz, observed in water	4.7	7.2
Calculated α in water, from Eqn. 19	1.62	0.73
Observed α in water, from Figure 11	1.61	0.37
Observed h, from Figures 10, 11	0.03	0.03

Table 1: TABLE 1. HIG Shaker Table Test Parameters

estimated then large errors in predicted amplitude and phase response can result. Uncertainties at frequencies above the coupling frequency resulting from the variation of the coefficients ω_c' and Q' are also likely.

3.2 Field Tests

Several major field experiments have been conducted within the past few years to test the coupling characteristics of existing OBSs. The first (and largest) was the Lopez Island OBS Intercomparison Test conducted during the summer of 1978, during which the characteristics of twelve OBSs were studied [Sutton et.al. (1981b)]. A second large cooperative test, conducted in Brest, France, was mainly for European groups [Snoek et.al.(1982)]. Three smaller tests were conducted by the Hawaii Institute of Geophysics in Keehi Lagoon, Oahu, in 1981, 1982 and 1985, to test modifications made to instruments suggested by the results of Lopez. Trehu (1985a) reported results of tests on the OBS used by the U.S. Geological Survey. The primary test in each case was the float transient test explained earlier. In addition, a series of shots were fired to supply seismic sources in some of the tests. In this paper we restrict the discussion to the transient test results.

Instrument parameters and results from the transient tests are given in Table II. *T 2*

NAME	M_i kg	M_w kg	r m	f_c Hz	Q_{obs}	Q_{th}	v_s m/s	r_{opt} m	$f_{c\ max}$ Hz	M_v, kg disk	sphere	cyl.	M_i^* kg	α
BL	10.3	5.2	.05	20.	3.5	3.2	18.1	.13	29.1	0	0	2.4	12.7	.60
SPL[1]	14	7.9	.06	22.	.5	2.6	19.6	.13	27.8	0.5	0	0	14.5	.58
MITEL	17	8.5	.24	21.	1.6	.29	20.3	.16	22.3	11.3	0	0	28.3	.70
NDL[1]	25	25	.18	17.		.76	17.7	.19	19.2	0	19	0	44	1.00
UTGL	69	46	.09	9.9	8.0	4.1	20.1	.26	13.9	11.4	35.5	0	116	.80
USGSL	118	93	.21	8.4	11.1	1.4	15.7	.32	11.5	13.1	72.8	0	204	.88
POL	150	115	.15	7.1		2.6	15.9	.33	11.1	4.8	0	75	230	.85
UWL	144	128	.05	4.6	7.7	15.0	18.7	.35	10.6	0	120	0	264	.94
BIOL	135	101	.34	9.9	3.5	.72	19.0	.35	10.4	55.5	0	85.5	276	.88
UCSBL	170	143	.26	9.	7.7	1.2	18.3	.36	10.3	24.8	4(15)	33.3	288	.91
SIOL	190	133	.31	11.	5.3	1.0	23.4	.38	9.6	42.1	120	0	352	.84
PSL	140	108	.56	19.	3.6	.31	43.6	.40	9.3	248	0	0	388	.92
OSUL	232	182	.39	8.1		.72	17.8	.40	9.1	83.8	2(35.5)	27	414	.88
LDGOL	250	150	.08	3.6		9.6	15.0	.41	8.9	0.7	2(51)	91	443	.77
UWFL	530	300	.20	3.9	2.9	3.0	13.3	.48	7.6	60.6	120	0	711	.68
B1	8.0	4.7	.05	15.	0.5	3.2	12.4	.12	31.1	0	0	2.4	10.4	.68
PD1	20.8	8	.28	25.	1.0	.33	29.1	.20	18.2	31	0	0	52	.75
L1	37.0	5	.29	15.	.5	.39	19.0	.22	16.3	34.5	0	0	71.5	.55
PO1	150	115	.15	9.5	6.	2.6	21.3	.33	11.1	4.8	0	75	230	.85
PN1	150	115	.28	12.	1.5	0.99	22.9	.34	10.7	31	0	75	256	.86
PS1	140.	108	.56	10.5	3.0	.31	24.1	.40	9.3	248	0	0	388	.92
B2	8	4.7	.05	22.5	1.5	3.2	18.5	.12	31.1	0	0	2.4	10.4	.68
OSU32	10.5	9.0	.20	17.0	1.5	0.37	14.6	.15	24.3	11.3	0	0	21.8	.93
L2	33	6.0	.29	11.0	2.0	0.39	13.7	.22	16.7	34.5	0	0	67.5	.60
OSU22	188	165	.40	15.0	2.0	0.52	31.9	.39	9.4	90	2(35.5)	27	376	.93
PS2	140	108	.56	11.0	2.3	0.31	25.2	.39	9.3	248	0	0	388	.92
OSU12	232	182	.39	14.0	2.0	.72	30.8	.40	9.1	83.8	2(35.5)	27	414	.88

[1] Some parameters for NDL (neutral density sphere buried in sediment) and SPL (buried spike) are calculated using sediment rather than water densities.

Table 2: Field Test OBS Parameters

The instrument masses, equivalent radii of the area in contact with the bottom, and mass of the water displaced by the OBS are all quantities dependent only on instrument design. Q_{th}, r_{opt}, f_{cmax}, M_v, M_i^*, and α are obtained from instrument parameters and an assumed sediment density of $\rho_s = 1570 kg/m^3$ and sediment velocity of 20 m/s. f_c, Q_{obs}, and v_s are obtained from the response of the vertical geophone in each OBS to a vertical float transient test, and equations presented above. An explaination of each parameter in the table is given below:

NAME: Name of OBS tested using the acronyms from the LOPEZ Experiment. Names ending in "L" are from the LOPEZ Experiment, names ending in "1" and "2" are from tests in Keehi Lagoon, Oahu, in 1981 and 1982. Instruments are listed in groups by experiment, and by increasing dynamic mass within experiments.

M_i: Instrument mass in kg.

M_w: Mass of water displaced by the instrument.

r: Equivalent radius of the area in contact with the sediment.

f_c: Coupling resonance frequency (and Q) are measured by comparison of spectra from transient tests with theoretical spectra from equation 24. An example is shown in Figure 12. *FIG 12*

Q_{obs}: Quality factor of the coupling frequency resonance peak measured from spectral analysis of the transient test data.

Q_{th}: Quality factor of the coupling frequency resonance peak from Equation 7.

v_s: Shear velocity of the sediments calculated from Equation 8.

r_{opt}: Optimum radius for area in contact with the sediment calculated from Equation 12 with M_i replaced by M_i^*.

$f_{c\ max}$: Maximum coupling frequency possible (at $r = r_{opt}$) from Equation 13.

M_v Virtual mass of water entrained in the motion of the OBS. This mass depends on the shape of the OBS, and is estimated by summing the contributions of different parts of the OBS, including the water above the area in contact with the sediment ($4\rho_w r^3/3$), the water around any spheres ($M_w/2$), and the water around any (horizontal) cylinders (M_w).

M_i^*: The dynamic mass of the OBS when emersed in water ($M_i^* = M_i + M_v$).

α: The coupling parameter defined by Equation 19.

From Equations 6, 8, and 9 we see that the quantity f_c/v_s, the coupling frequency divided by the sediment shear velocity, should be a simple function of the sediment density, the OBS bearing radius, and M_i^*. As normal sediment densities occur only within bounds from about 1300 to 1700 kg/m^3, this function is mainly determined by the dynamic mass ($M_i^* = M_i + M_v$) and the bearing radius (r) of the OBS. Thus, for a given OBS, a measurement of f_c should be directly proportional to the shear velocity. A plot of f_c/v_s calculated from Equation 6 (using an appropriate dynamic mass and radius from Table II) versus f_c measured from transient test spectral data (Table II) is shown in Figure 13. Each point represents the average of several coupling frequency measurements *FIG 13* at either Lopez Island or Keehi Lagoon. The shear velocity of the sediment beneath each OBS can be estimated for each point by dividing the observed f_c by the predicted f_c/v_s. Although there is considerable scatter, note that all but a few of the 27 points lie between 15 and 30 m/s, and, as two different sites are represented and each OBS was in a slightly different location, much of the scatter is probably the result of real variations in shear velocity. There is no obvious correlation of shear velocity with instrument mass or bearing radius, suggesting that the theory successfully accounts for changes in these parameters. Note that (with the exception of the Plate Standard, having a mass of 140 kg when tested at Lopez Island) all OBSs with observed coupling frequencies above 15 Hz have masses less than 50 kg, and all OBSs with coupling frequencies less than 10 Hz have masses greater than 100 kg. OBSs with masses that differ by more than an order of magnitude yield estimates of shear velocity that agree within a factor of 2, suggesting some validity for the theory.

The same data are presented in Figure 14 in a different way. In Figure 14, using the relationships *FIG 14* in Table II, the ratio of observed f_c to $f_{c\ max}$ is plotted versus the ratio of actual radius to optimum radius. The theoretical curve is shown for comparison. As for the preceeding figure, much of the scatter probably results from real variations in sediment shear velocity.

Q' of the coupling resonance at f_c as predicted by Equation 7 is plotted versus observed Q' in Figure 15. It is noted that the predicted Q' is lower than the observed Q' in most cases, which *FIG 15* means that most OBSs "bounce" at the coupling frequency more than is predicted from the half-space theory. Note that all but one observed Q' value above 2. are from large-mass OBSs, and all but one Q' value less than 2 are from small-mass OBSs. Thus, although the theory does not match the observed values of Q', the desirability of a low Q' coupling resonance still leads us to the same conclusion: that small mass OBSs perform better than large mass OBSs. The reason the theory does so poorly in modeling Q' is not known; however, there are several possibilities. The theory assumes that the sediment is a homogeneous half space, but velocity generally increases with depth. This gradient should be "felt" by the more massive OBSs with the greater bearing radii and with the lower coupling frequencies. Energy would not radiate away from the system as fast as predicted by the half-space theory, in agreement with the layered theory of [Luco (1974)]. The smaller OBSs would not feel as deeply.

4 OBS DESIGN PARAMETERS

On the basis of the theory and observations discussed above, an ocean bottom seismometer shou. be designed with the following constraints:

1. minimum mass,

2. radius in contact with the ocean floor given by equation 12 (with M_i replaced by M_i^*), and radius less than 1/4 of the shear wavelengths, and

3. density approximately that of the sediment.

In addition, the following constraints will minimize rocking modes, cross coupling, and noise coupled to the OBS by motion of the water:

4. low height-to-base area ratio, low moment of inertia about horizontal axes, and small (smooth) cross section with the water, and

5. low density gradients, and maximum symmetry about the vertical axis.

Each of the above constraints is discussed below:

1). As data near and above the coupling frequency are potentially distorted by motion of the OBS relative to the sediment, it is advisable to keep this frequency as high as possible by minimizing the OBS mass. On land (and in the ocean where there is no sediment cover) this is generally not a problem because shear velocities are usually high enough to move the coupling frequency above the range of interest.

Note that while this analysis is done for vertical coupling, a similar analysis can be done for horizontal coupling. As there are more degrees of freedom in horizontal coupling, the situation is more complicated. Horizontal transient test data suggest that the coupling problem is more severe in the horizontal direction than in the vertical, and that values of Q' are higher and coupling frequencies are lower. The small-mass (moment of inertia) guideline still holds, however, since the same parameters are involved. Note also that Q' tends to increase with increasing mass (Figure 15), and that low Q' at coupling resonances is also desirable.

If mass is not minimized, the response of the OBS in the seismic frequency band will potentially vary with shear velocity of the near-bottom sediments. Although, as mentioned earlier, it is possible to make in situ calibrations using internally generated transients, the relationship between the seismic response and transient test response will be in doubt (for instance, if the OBS is not

vertical). According to the theory, if the OBS has the same density as the surrounding material, it should not be affected by coupling as long as the seismic wavelengths are much larger than the OBS (see 3 below).

2). If the equivalent radius of the area in contact with the sediment is not optimal, then the coupling frequency will be lower than the best possible value for that mass of OBS (M_i^*) and sediment density (Figure 3). OBSs with relatively small radii with respect to their mass, (such as LDGOL and UWL in Table II) have low coupling frequencies, and PS1 and PS2, with relatively large radii, also show low coupling frequencies. Only three OBS tests (PSL, OSU12, and OSU22) show coupling frequencies significantly higher than expected from the OBS characteristics and those of the sediments. The reason is unknown, but they may have been resting on stiffer sediment or rocks. Trehu (1985a) reports results of in-situ transient tests on OBSs of differing mass and base radius. These tests are for configurations with ratios of mass-to-base radius greater than those covered by the second order approximation to K and R given in equations 4 and 5. Her observed resonant frequencies are compatable with a zero order theory where $\omega_c = (K_0/M_i^*)^{1/2}$, which she prefers to the second order theory. With the zero order theory, the curves shown in figures 3 and 14 become straight lines coincident with the lines in the figures for small radii. Trehu points out that the flexibility of the OBS base can lead to lower damping and a marked decrease in the frequency dependance of K. Also, anelastic attenuation within the sediments should lead to a decrease in the variation of the spring and damping coefficients with frequency. However, the second order theory seems to fit our (more numerous) data better than the zero order theory.

3). If the density of the OBS is the same as that of the surrounding medium, then the OBS is neutrally bouyant and the OBS should move with its surroundings for seismic inputs regardless of coupling effects. An instrument with a low vertical profile and density equal to that of the sediment should move with the sediment. This is not true if the OBS dimensions are larger than a fraction of a wavelength, because the velocity of a seismic wave through the OBS will not be the same as the velocity in its surroundings, and the OBS will distort the motion. This distortion is especially

important for OBSs on sediment since, for example, if $v_s = 10\ m/s$, the wavelength at 20 Hz is only 0.5 m. Thus, even with neutral density, distortion can be expected at higher frequencies.

The adverse effects of coupling increase as the OBS density increases above the sediment density as shown in Figure 7. If care has been taken to insure that all coupling resonances are well above the frequencies of interest, then density will not be a problem, but designing for neutral density will add insurance for having a predictable and smooth transfer function.

4). Low profile and small cross section in the water. In many situations, the ocean water and the sediments have a discontinuity of horizontal particle motion at the ocean floor. This is obvious in the case of significant ocean currents [Duennebier et.al. (1981),Trehu and Solomon (1981)], but this discontinuity can also be a problem for seismic inputs, especially shear waves. If most of the volume of the OBS is in the water, the instrument will tend to move with the water rather than with the sediment. The water and sediment move together for vertically incident compressional energy, but for other angles of incidence and wave types they do not. The bottom of an OBS with a large cross section in the water will tend to move with the sediment while the top will tend to move with the water. This torquing will most likely result in detected motion that is severely distorted, with horizontal particle motion recorded by the vertical sensors. If the vertical profile of the OBS is as low as possible and the base-to-height ratio is large, this problem should be eliminated. A lower vertical profile will produce a lower rocking mode sensitivity and a higher rocking mode coupling frequency. However, increasing the vertical cross section within the sediment should improve the response to horizontal particle motion.

5). OBS symmetry and minimum density gradients will tend to reduce distortion caused by cross coupling. An OBS with its sensors located at the vertical axis of symmetry between the center of buoyancy and the center of mass will give a minimum of cross coupling problems. As noted earlier, the center of buoyancy and center of mass should be as close as possible to avoid torquing due to density gradients in the package. If the OBS is elongated in one horizontal direction it will be less sensitive to cross coupling in that direction. If the geophones are located off the axis

of symmetry they will be more sensitive to rocking and twisting modes of motion of the package [Luco (1974)]. Changes in shape in any direction will modify the response, as virtual mass is very shape dependent, thus maximizing symmetry is desirable.

4.1 Practical Considerations

The geophones must be separated from the necessarily massive package that contains power, electronics, recording, and recovery equipment to obtain OBS masses that are as small as possible. Although this separation may add some complexity, and possibly lower reliability than when everything is in one package, we believe that the advantages of the increase in signal fidelity due to minimization of coupling problems, the likely decrease in noise from water currents and recording equipment [Bycroft (1956),Duennebier et.al. (1981)], and the flexibility in sensor configurations, far outweigh the disadvantages.

Separation of the geophones and the recording package requires an electro-mechanical connection between the sensors and the recording package. A preamplifier is desireable for each sensor in the geophone package to prevent problems caused by electrical leakage to sea water in the cable and connectors. The cable is also a potential problem if it should get caught under the OBS ballast, and thus prevent the instrument's return. This problem can be reduced by replacing the traditional solid anchor with particulate ballast that the cable can pass through when the ballast is released. The recording package itself can be a source of seismic noise and signal distortion through reradiation of current and seismic inputs. Careful design and adequate separation from the sensor package can eliminate this problem.

As geophone packages get smaller, other problems are likely to be encountered because of the decreased mass. One of these problems is the electro-mechanical connection to the recording package. This link must be carefully designed to prevent mechanical forces on the cable from being transmitted to the sensor package.

5 CONCLUSIONS

In this paper we have presented theoretical arguments and data that suggest that ocean bottom seismometers should be designed to be as small as possible to prevent poor signal fidelity caused by coupling problems. In addition, there is an optimum surface area in contact with the sediment depending on the OBS mass, shape, and sediment density. It is found that the frequency above which seismic signals are distorted is directly proportional to the sediment shear velocity. We conclude that significant improvement in the quality of seismic data can be made if the guidelines presented in this paper are followed in the design of future ocean bottom seismometers.

6 ACKNOWLEDGMENTS

The field programs at Keehi Lagoon were orchestrated and conducted by the HIG Engineering Support Facility; our special thanks to all personnel involved for their efforts. Dale Bibee, Oregon State University, supplied the digital recording system for the 1982 Keehi test and supplied three of the OBSs. The manuscript has been edited by Rita Pujalet, HIG Publications, and reviewed by R. Cessaro and Patrica Cooper. All of this research, from LOPEZ to this publication, was funded by the U.S. Office of Naval Research. HIG Contribution No. 00000.

7 figure captions

Figure 1. F_1 and F_2 vs. dimensionless frequency (a) from equations 5 for a circular disk in contact with the sediment. The points on the curves are from an analytical solution by Bycroft (1956). The optimum dimensionless frequency is shown by the dashed line.

Figure 2. Effective mass ($M'/M_i = \frac{4}{4-a_c^2}$) and damping coeficient ($h = \frac{6.9a_c}{16-4a_c}$) vs. dimensionless resonant frequency a_c for a circular disk-shaped OBS. The optimum coupling frequency occurs at $a_c = 1.16$, shown by the dashed line.

Figure 3. The ratio of coupling frequency to sediment shear velocity vs. bearing radius for circular disks with different masses (M_i). When the OBS is immersed in water, M_i is replaced by the dynamic mass, $M_i^* = M_i + M_v$. The curves terminate at the limit of reliable second order theory.

Figure 4. Increase in r_{opt} and decrease in $f_{c\ max}$ with increasing mass for a circular disk from Equations 12, and 13.

Figure 5. The ratio of motion v_i of a sphere of density ρ_i to that of surrounding water, v_w, as a function of the ratio of sphere mass, M_i, to the mass of water displaced by the sphere, M_w, from equation 14. When the sphere density is zero, its motion is three times that of the water.

Figure 6. The ratio of motion of a disk, v_i, to that of surrounding water, v_w, as a function of the ratio of disk radius r, to the disk thickness, t, from equation 15. The water is moving in a direction perpendicular to the plane of the disk.

Figure 7. Theoretical seismic phase and amplitude response for three values of α for $h = 0.1$ from equations 21 and 22. These curves are do not depend on OBS shape.

Figure 8. Theoretical seismic phase and amplitude response for three values of h for $\alpha = 0.5$ from equations 21 and 22.

Figure 9. Schematic drawing of shaker table coupling experiment. The table motion is monitored with geophone R, and the motion of a sphere suspended by a spring is monitored by an identical geophone (T) inside the sphere. A, vertical tests; B, horizontal tests.

Figure 10. Seismic phase and amplitude response of a sphere suspended in air. The smooth curves are solutions to Equations 21, and 22 for the spheres using the appropriate parameters from Table 1. Figures 10a and b are for vertical motion of a sphere less dense than water, and 10c and d are for horizontal motion of a sphere more dense than water.

Figure 11. Seismic phase and amplitude response of a sphere suspended in water. The smooth curves are solutions to Equations 21 and 22 for each sphere using the appropriate parameters from Table 1. Figures 11a and b are for vertical seismic motion of a sphere less dense than water, and 11c and d are for horizontal seismic motion of a sphere more dense than water.

Figure 12. Example of the comparison between theoretical response of an OBS to a vertical transient test, and the actual response of a geophone (dashed line is from Equation 24). The noise spectrum is shaded. The time domain curve is also shown. Care must be taken in these comparisons to correct for the geophone response.

Figure 13. Theoretical ratio of the coupling frequency to the sediment shear velocity (f_c/v_s), compared with observed coupling frequencies, (f_c), from vertical transient tests. f_c/v_s is calculated using equation 6 and appropriate parameters from Table 2. Each symbol represents the average of several vertical transient tests for a particular OBS at either Lopez Island (squares), the 1981 Keehi Lagoon test (triangles), or the 1982 Keehi test (diamonds). The symbol size is proportional to the log of the appropriate dynamic mass from Table II. Each point can be used to estimate the shear velocity of the sediment below the OBS. The two lines are iso-velocity lines at 15 and 30 m/s.

Figure 14. $f_c/f_{c\ max}$ vs. the ratio of the radius of the area in contact with the sediment to the optimum radius. The data points are from Table 2 (assuming that $\rho_s = 1570 kg/m^3$ and $v_s = 20 m/s$), and the theoretical curve obtained from equations 6, 12 and 13, is independent of sediment parameters. $f_c/f_{c\ max} = 1.73[\frac{r/r_{opt}}{2+(r/r_{opt})^3}]^{1}/2$. Dashed line is the limit of reliable second order theory.

Figure 15. Theoretical Q from Equation 7 versus measured Q. Note that high values of Q are observed only from large OBSs.

References

[Arnold et.al. (1955)] Arnold, R.M., G.N. Bycroft, and G.B. Warburton: 1955. 'Forced vibrations of a body on an infinite elastic body', J. Appl. Mech., Trans. ASME, v. 77, p. 391-401.

[Bachelor (1967)] Batchelor, G. K.: 1967, An Introduction tc Fluid Dynamics, Cambridge University Press, 615 p.

[Bycroft (1956)] Bycroft, G.N.: 1956,'Forced vibrations of a rigid circular plate on a semi-infinite elastic space and on an elastic stratum', Phil. Trans. Roy. Soc. Lond., V248 A928, p. 327-367.

[Byrne et.al. (1983)] Byrne, D. A., Sutton, G. H., Blackinton, J. G., and Duennebier, F. K.: 1983, 'Isolated Sensor Ocean Bottom Seismometer', Marine Geophys. Res., 5, 437-449.

[Duennebier et.al. (1981)] Duennebier, F. K., Blackinton, J. G., and Sutton, G.: 1981, 'Current-Generated Noise Recorded on Ocean Bottom Seismometers', Marine Geophys. Res., 5, 109-115.

[Duennebier and Blackinton (1983)] Duennebier, F. K., and Blackinton, J. G.: 1983, 'The Ocean Sub-Bottom Seismometer', in CRC Handbook of Geophysical Exploration at Sea, CRC Press, Boca Raton, Florida, 317-332.

[Duennebier et.al. (1984)] Duennebier, F.K., G.H. Sutton, D. Harris, and D. Byrne: 1984, 'A Simple Shaker Table for Seismometer Calibration', Marine Geophys. Res., 6, p. 311-328.

[Duschenes et.al. (1981)] Duschenes, J. M., Barash, T. W., Mataboni, P., and Solomon, S.: 1981, 'On the Use of an Externally Deployed Geophone

Package on an Ocean Bottom Seismometer', Marine Geophys. Res., 4, 437-450.

[Hsieh (1962)] Hsieh, T. K.: 1962, 'Foundation Vibrations', Proc. Inst. Civ. Eng., 22, 211-226.

[Koelsch and Purdy (1979)] Koelsch, D., and Purdy, G. M.: 1979, 'An Ocean Bottom Hydrophone Instrument for Seismic Refraction Experiments in the Deep Ocean', Marine Geophys. Res., 4, 115-125.

[Krohn (1984)] Krohn, C.E.: 1984, Geophone Ground Coupling, Geophysics, 49, 722-731. Lewis, B., and Tuthill, J.: 1981, 'Instrumental Waveform Distortion on Ocean Bottom Seismometers', Marine Geophys. Res., 5, 79-86.

[Luco (1974)] Luco, J. E.: 1974, 'Impedance Functions for a Rigid Foundation on a Layered Medium', Nuc. Eng. Des., 31, 204-217.

[Milne-Thompson (1950)] Milne-Thompson :1950, Theoretical Hydrodynamics, MacMillan, N.Y., 600 p.

[Safar (1978)] Safar, M. H.: 1978, 'On the Minimization of the Distortion Caused by the Geophone Ground Coupling', Geophysical Prospecting, 26, 538-549.

[Snoek et.al.(1982)] Snoek, M., C. Bottcher, and W. Schneider, 'OBSCAL Report, Ocean Bottom Seismometer Intercalibration and Coupling Experiment', University of Hamburg.

[Sutton et.al. (1981a)] Sutton, G. H., Duennebier, F. K., and Iwatake, B.: 1981a, 'Coupling of Ocean Bottom Seismometers to Soft Bottom' ,Marine Geophys. Res., 5, 35-51.

[Sutton et.al. (1981b)] Sutton, G. H., Duennebier, F. K., Iwatake, B., Tuthill, J., Lewis, B., and Ewing, J.: 1981b, 'An Overview and General Results of the Lopez Island OBS Experiment', Marine Geophys. Res., 5, 3-34.

[Trehu (1985a)] Trehu, A.M.: 1985a, 'Coupling of Ocean Bottom Seismometers to Sediment: Results of tests with the U.S. Geological Survey Ocean Bottom Seismometer', Bull. Seism. Soc. Am., 75, 271-289.

[Trehu (1985b)] Trehu, A.M.: 1985b, 'A note on the effect of bottom currents on an oecan bottom seismometer', Bull. Seism. Soc. Am., 75, 1195-1204.

[Trehu and Solomon (1981)] Trehu, A., and Solomon, S.: 1981, 'Coupling Parameters of the MIT OBS at two Nearshore Sites', Marine Geophys. Res., 5, 69-78.

[Zelikovitz and Prothero (1981)] Zelikovitz, S. J., and Prothero, W.: 1981, 'The Vertical Response of an Ocean Bottom Seismometer: Analysis of the Lopez Island Vertical Transient Tests', Marine Geophys. Res., 5, 53-67.

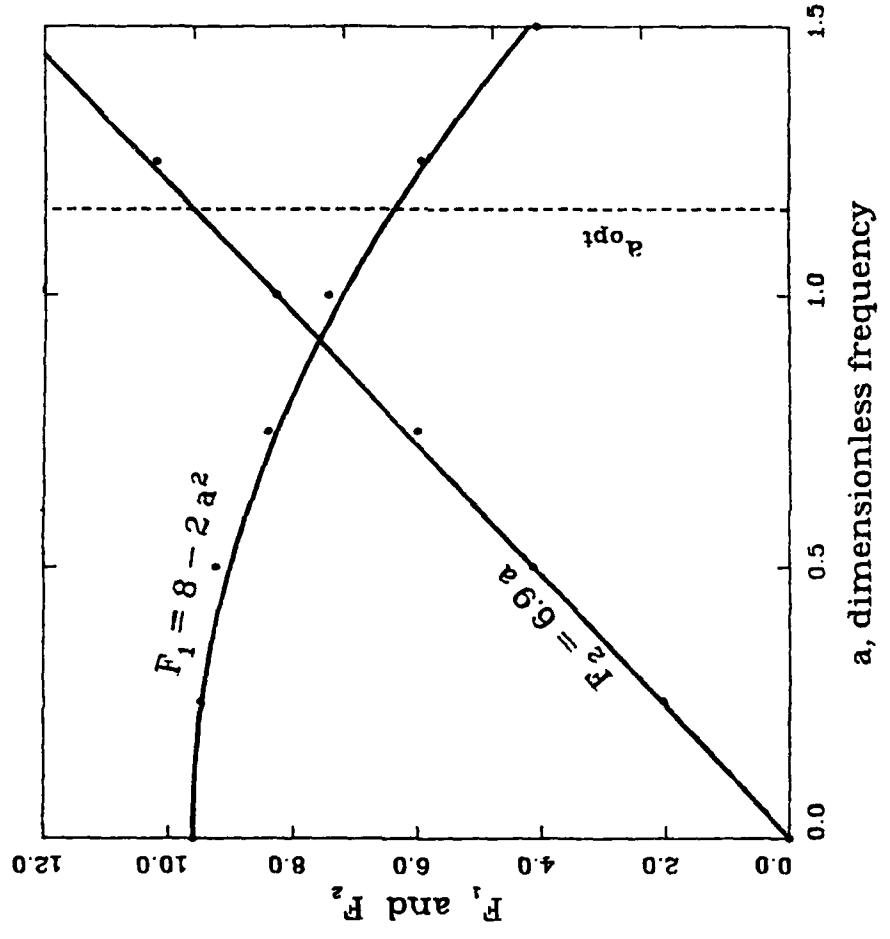
$F_1 = 8 - 2a^2$
$F_2 = 6.9a$
a_{opt}
F_1 and F_2
a, dimensionless frequency
0.0
2.0
4.0
6.0
8.0
10.0
12.0
0.0
0.5
1.0
1.5

Figure 1.

Figure 2.

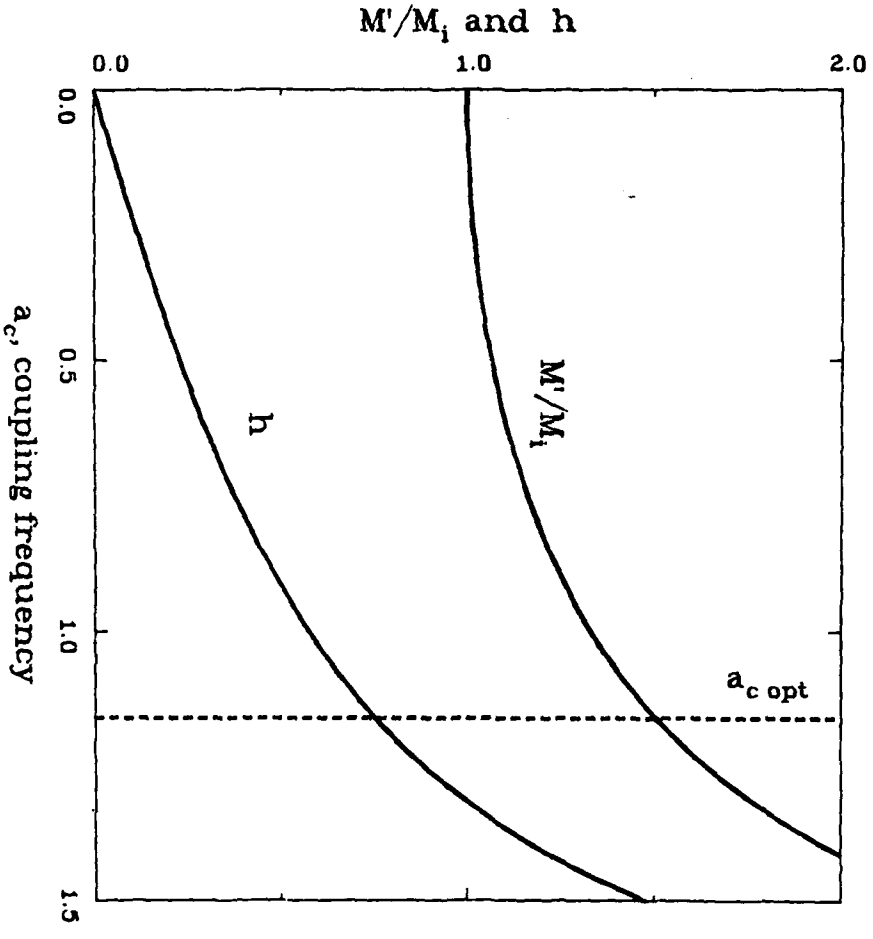

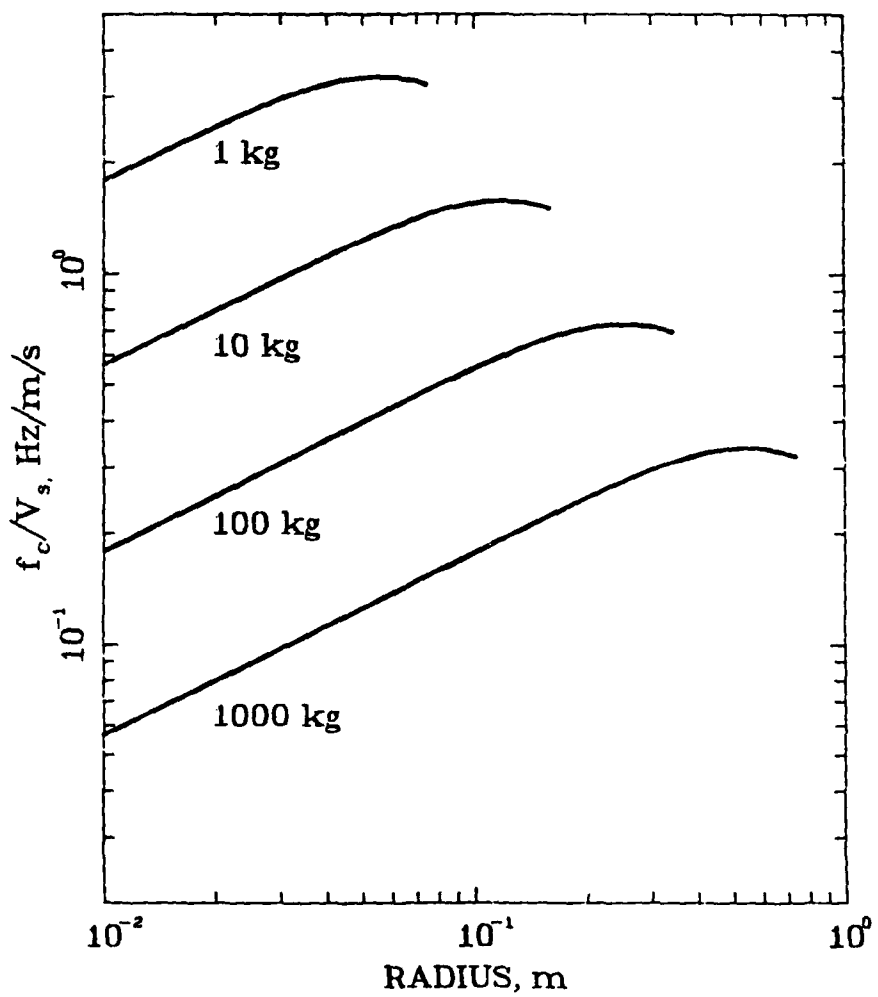

Figure 3.

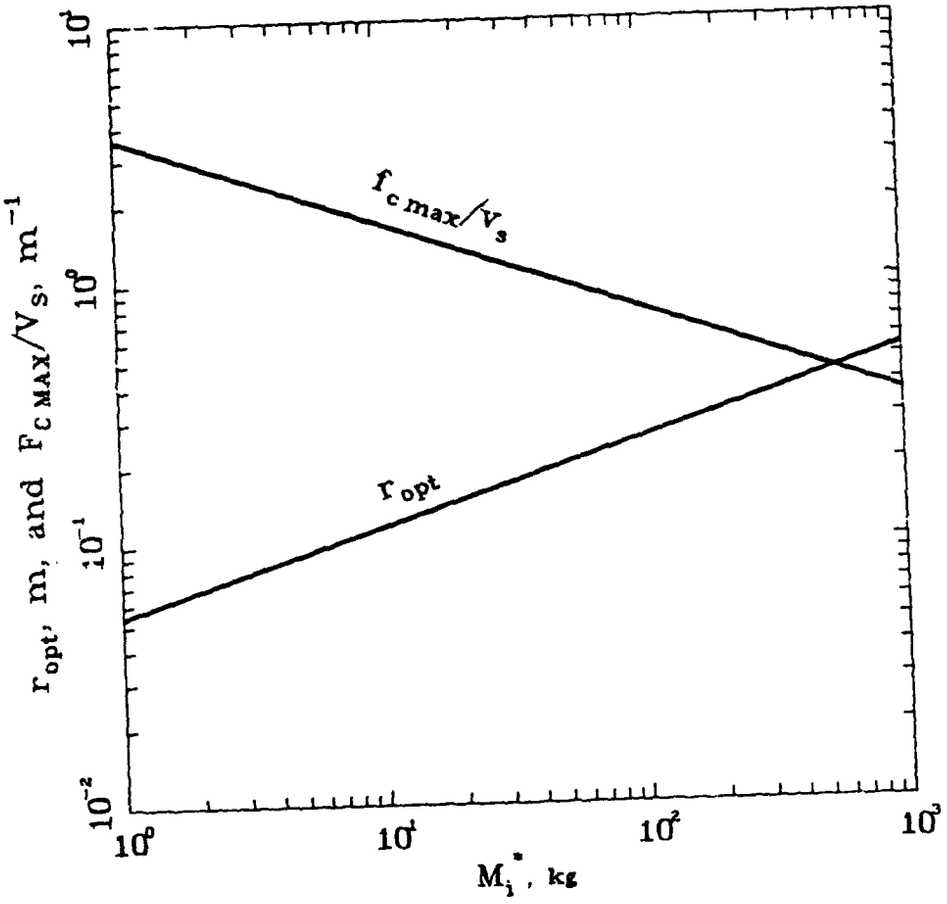
$f_{c\,max}/V_s$
r_{opt}
r_{opt}, m, and $F_{c\,MAX}/V_s$, m^{-1}
M_i^*, kg
10^1
10^0
10^{-1}
10^{-2}
10^0
10^1
10^2
10^3

Figure 4.

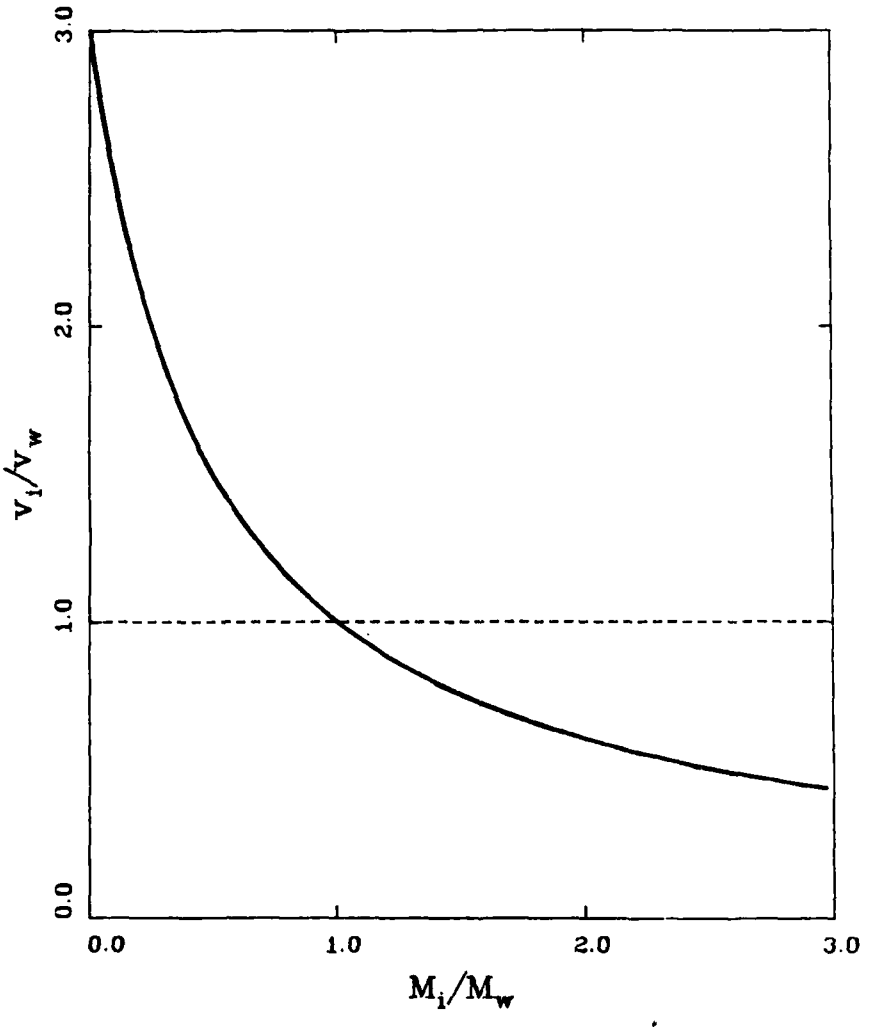

Figure 5.

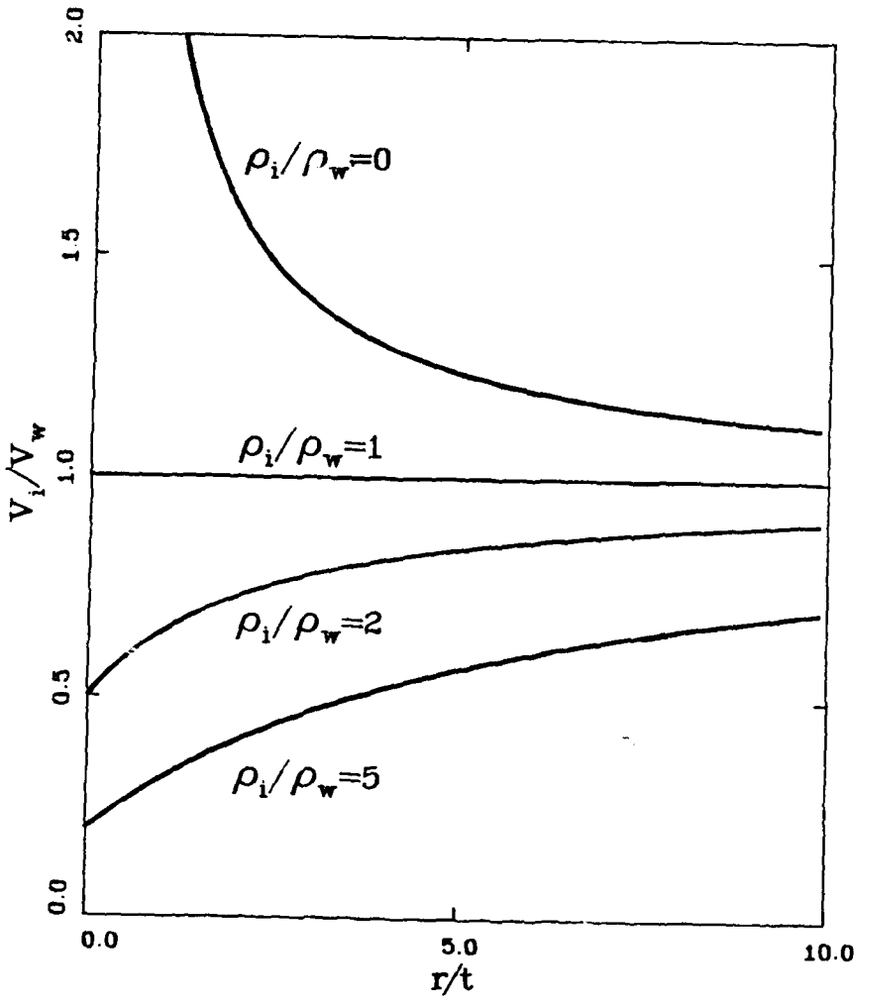
2.0
1.5
1.0
0.5
0.0
V_i/V_w
ρ_i/ρ_w=0
ρ_i/ρ_w=1
ρ_i/ρ_w=2
ρ_i/ρ_w=5
0.0
5.0
10.0
r/t

Figure 6.

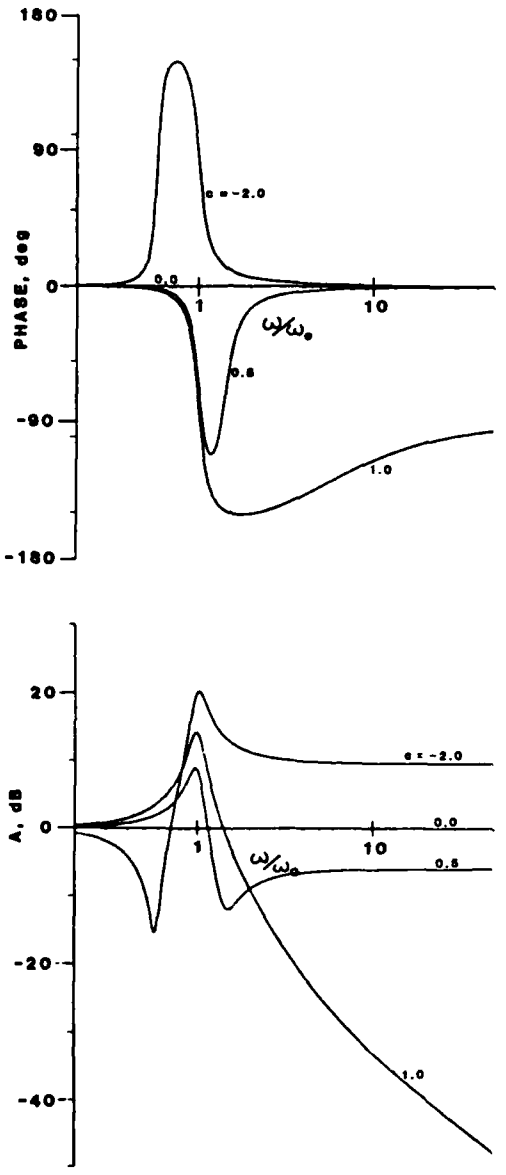
180
90
0
-90
-180
PHASE, deg
α = -2.0
0.0
0.5
1.0
1
10
ω/ω₀
20
0
-20
-40
A, dB
α = -2.0
0.0
0.5
1.0
1
10
ω/ω₀

Figure 7.

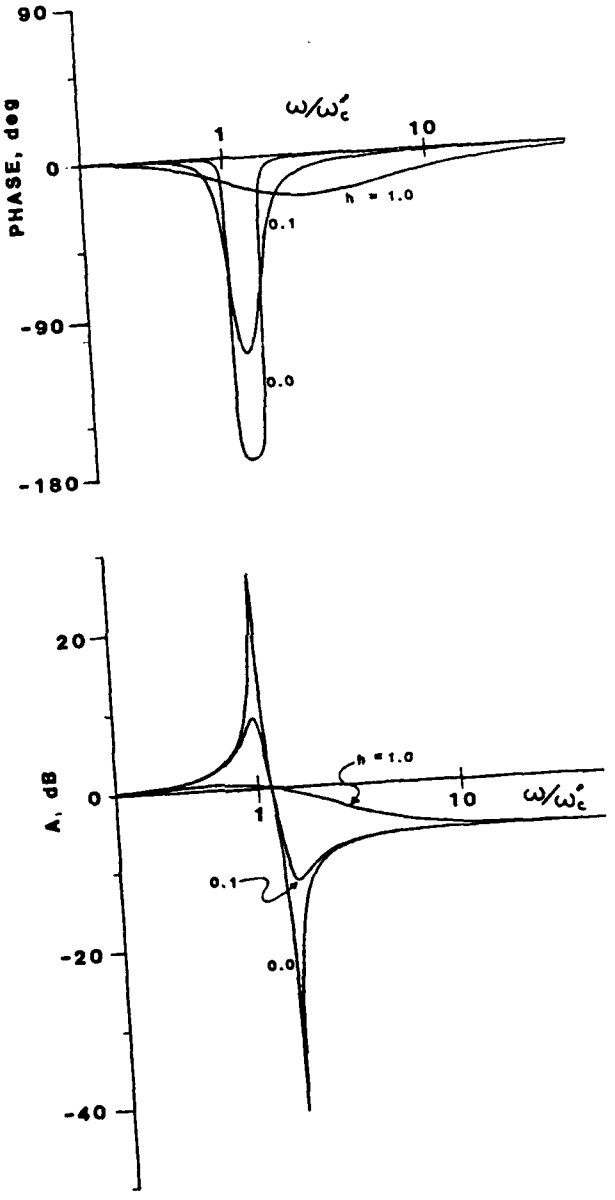
90
0
-90
-180
PHASE, deg
ω/ω'c
1
10
h = 1.0
0.1
0.0
20
0
-20
-40
A, dB
h = 1.0
1
10
ω/ω'c
0.1
0.0

Figure 8.

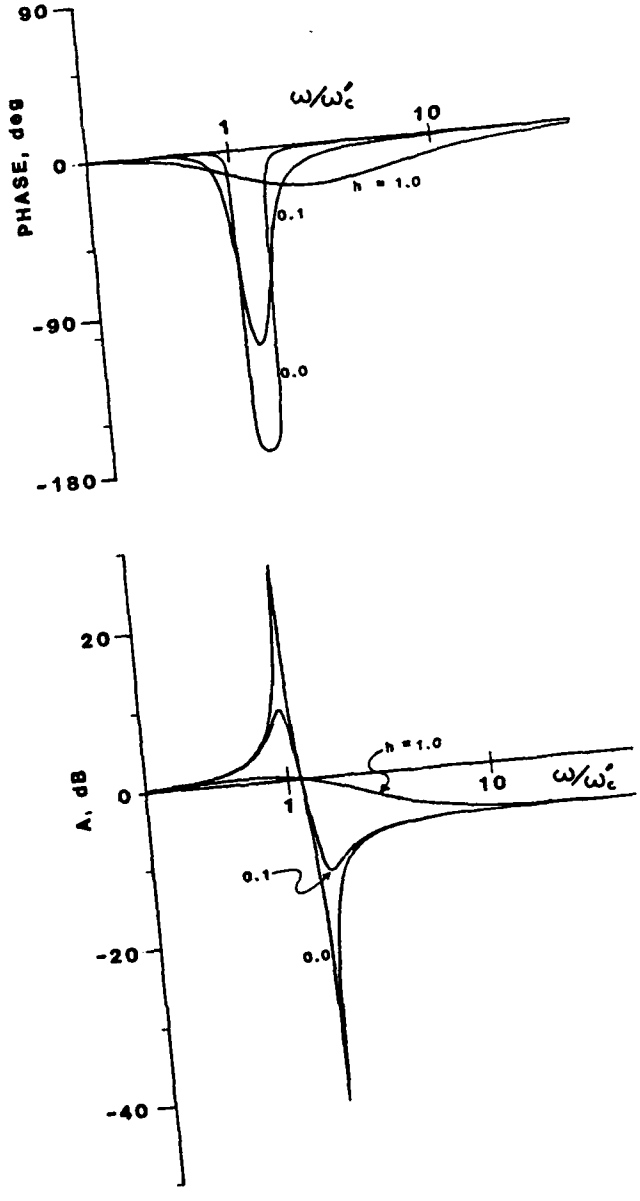
90
0
-90
-180
PHASE, deg
ω/ω'c
1
10
h = 1.0
0.1
0.0
20
0
-20
-40
A, dB
h = 1.0
ω/ω'c
1
10
0.1
0.0

Figure 8.

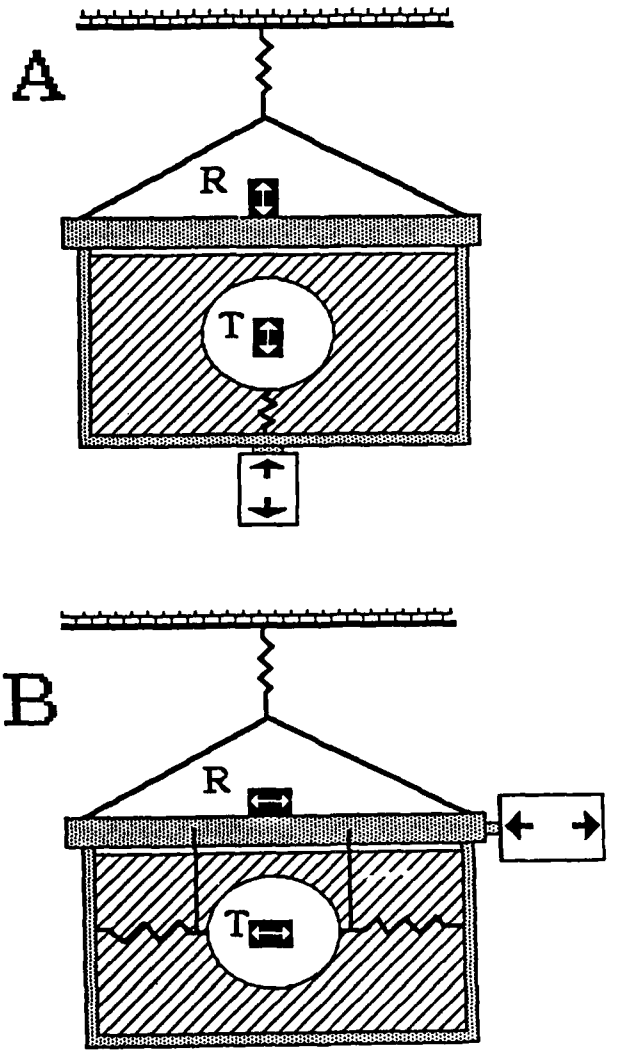

Figure 9.

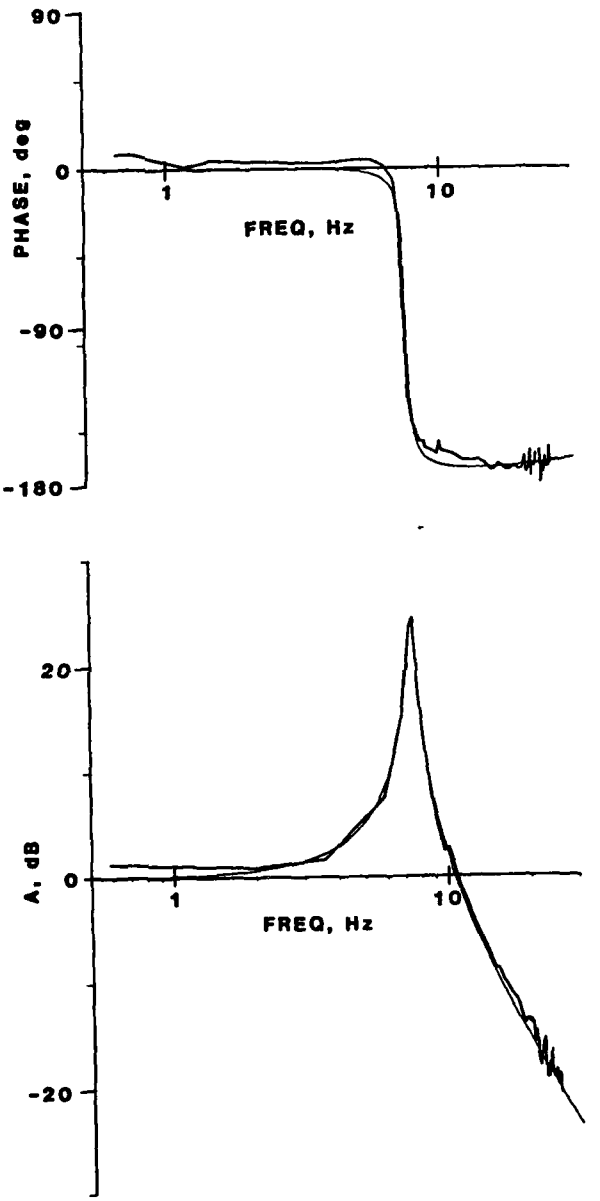

Figure 10.

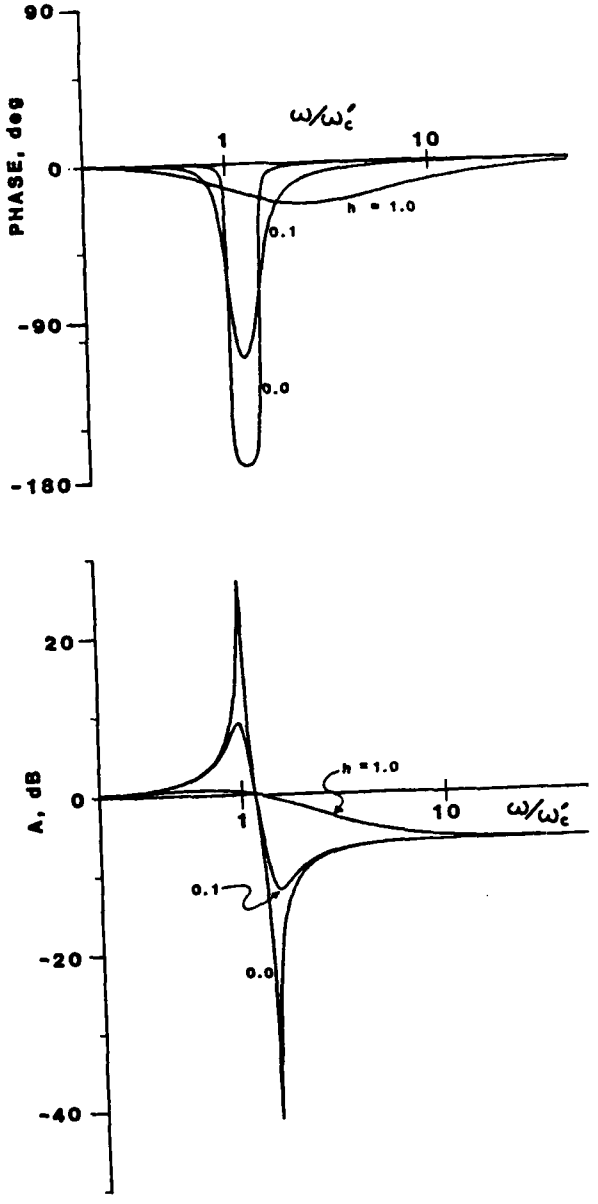
90
0
-90
-180
PHASE, deg
ω/ω'c
1
10
h = 1.0
0.1
0.0
20
0
-20
-40
A, dB
h = 1.0
1
10
ω/ω'c
0.1
0.0

Figure 11.

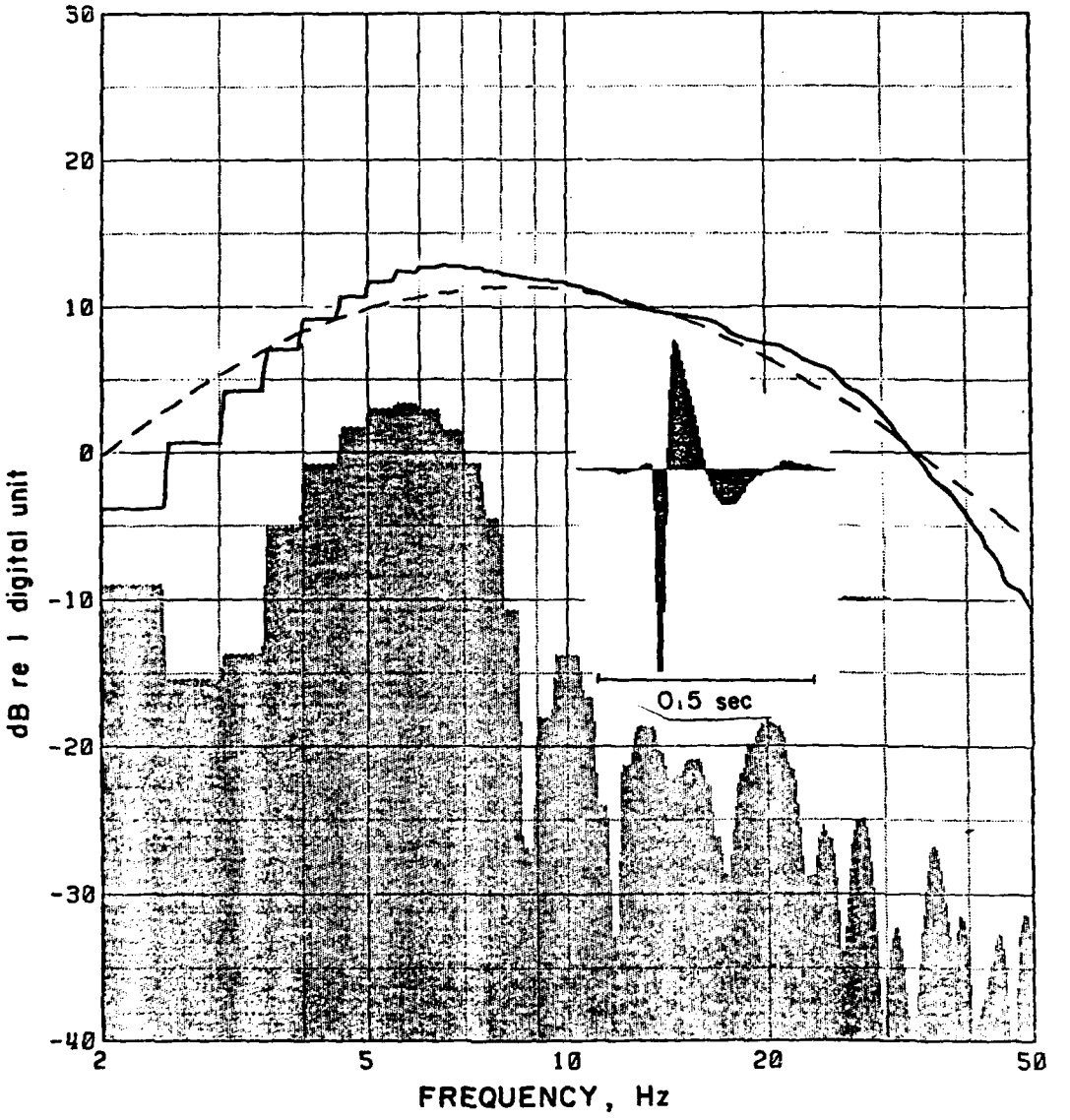
30
20
10
0
-10
-20
-30
-40
dB re 1 digital unit
0.5 sec
2
5
10
20
50
FREQUENCY, Hz

Figure 12.

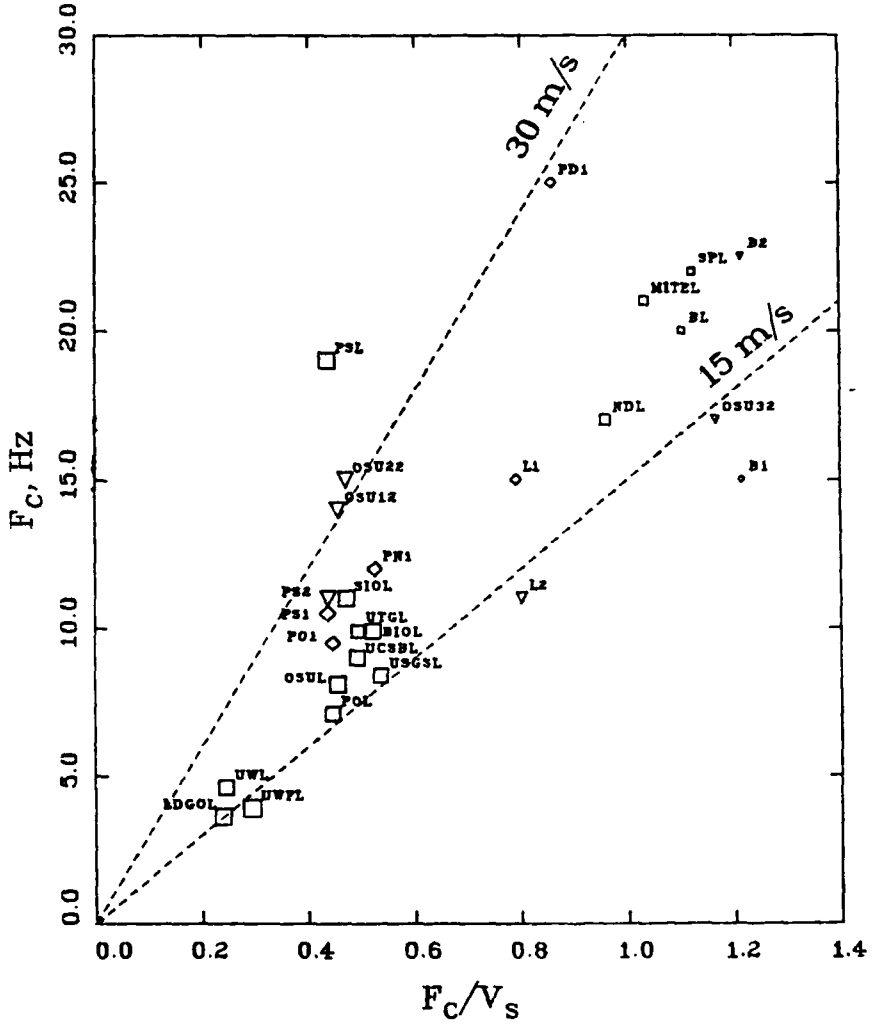
30 m/s
15 m/s
PD1
SPL
B2
MITZL
BL
PSL
NDL
OSU32
OSU22
L1
B1
OSU12
PN1
L2
BIOL
PS2
PS1
UTGL
BIOL
PO1
UCSBL
USGSL
OSUL
POL
UWL
UWFL
ADGOL
0.0
5.0
10.0
15.0
20.0
25.0
30.0
0.0
0.2
0.4
0.6
0.8
1.0
1.2
1.4
F_C, Hz
F_C/V_S

Figure 13.

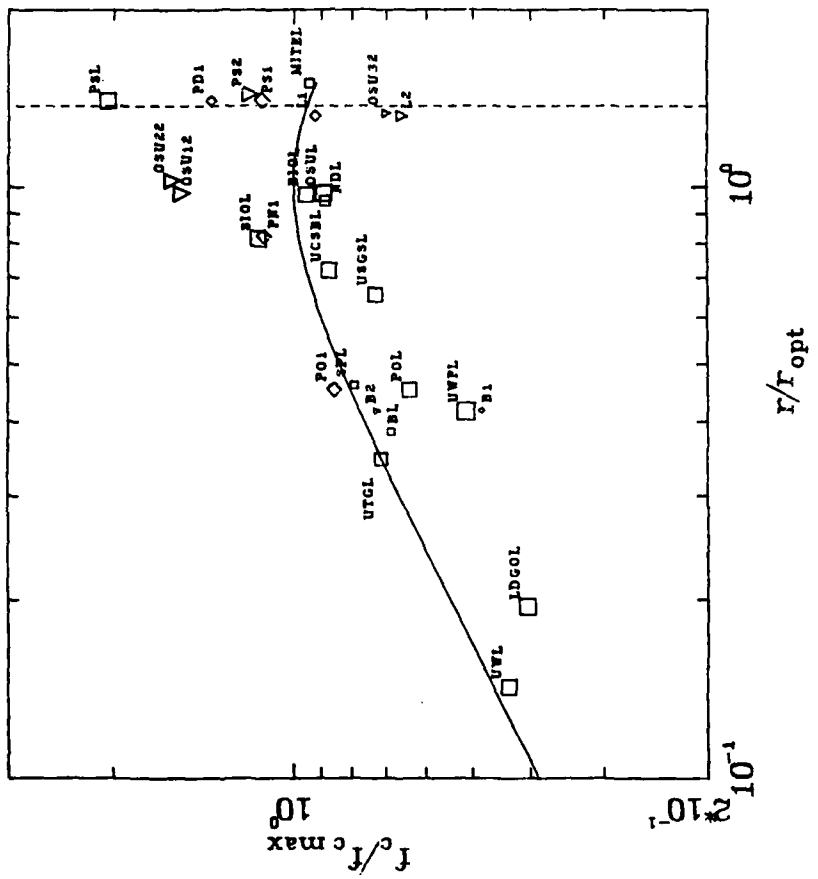
PSL
PD1
PS2
PS1
MITEL
OSU32
OSU22
OSU12
PIOL
PF1
OSUL
PDL
UCSBL
USGSL
PO1
P2
POL
UWPL
B1
OBL
UTGL
JDGOL
UWL
$f_c/f_{c\,max}$
10^0
$2*10^{-1}$
10^{-1}
r/r_{opt}
10^0

Figure 14.

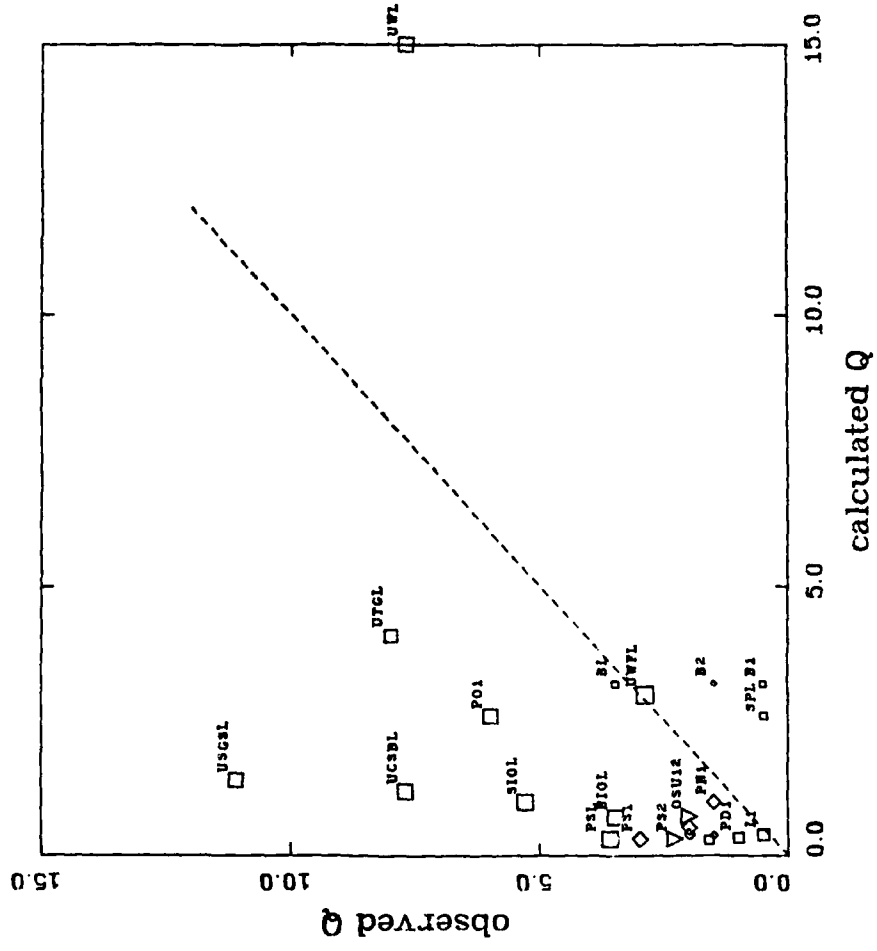
observed Q
calculated Q
0.0
5.0
10.0
15.0
UWL
UTGL
USGSL
UGSBL
PO1
SIOL
BL
UWPL
B2
SPL B1
PS1
BIOL
PS2
OSU12
PBL
PD1
LF

Figure 15.

From: OCEAN SEISMO-ACOUSTICS
Edited by Tuncay Akal and Jonathan M. Berkson
(Plenum Publishing Corporation, 1986)

OCEAN BOTTOM SEISMOLOGY: HISTORY AND CURRENT STATUS

George H. Sutton

Rondout Associates, Incorporated
P.O. Box 224
Stone Ridge, New York 12484 USA

ABSTRACT

Ocean bottom seismographs (OBS) have been in use for almost 50 years. The earliest instruments were used for short range explosion refraction experiments but were soon abandoned when techniques involving near surface sources and receivers were introduced. Development of OBS technology revived during the late 1950's inspired by interest in the detection and identification of clandestine nuclear explosions and supported largely by the VELA-UNIFORM program of the United States government. Since that time, OBS research has expanded to include over 25 organizations in several countries. Generally each group has developed its own instrumentation and experimental procedures. Instruments fall into four classes: (1) self-contained, free-fall, pop-up; (2) acoustically telemetering to near surface for retransmission or recording; (3) electrically telemetering via cable to the surface; and (4) permanently linked to shore by cable. Most fall in class (1). Sensor configurations range from a single vertical component (or hydrophone) to three-components plus hydrophone; seismometer free period is generally one second or less; frequency response is generally limited to 100 Hz or less. Instrument masses range from 60 to 600 kg, recording is analog (AM or FM) continuous or digital (time windowed and/or triggered); dynamic range, data storage capacity and deployment time all cover a wide range of values. Most applications are for determination of velocity structure and/or local seismicity. There has been lesser interest in teleseismic, engineering or strong-motion applications. Major problem areas or areas where improvements are needed include bottom-coupling (signal distortion) and noise; data storage; system reliability, especially over long deployment times; ease of handling during launch and retrieval; and ease of shipboard checkout before and after deployment. OBS have recently been supplemented by ocean subbottom seismometers emplaced beneath the sediment in a bore-hole.

INTRODUCTION

OBS operated at selected oceanic sites afford an opportunity to explore seismic wave propagation under the deep ocean basins and across continental and island margins; ambient seismic noise in the ocean basins, both natural and cultural; the generation of storm microseisms; and the distribution and mechanisms of local submarine earthquakes. In addition, OBS are required for uniform areal obse-vations of seismic waves from teleseismic events. As mentioned in the abstract, by far the majority of OBS have been of the pop-up variety, designed and used for relatively short term active and/or passive experiments.

The design of a good, reliable OBS is a challenging task. In addition to the requirements of any remotely operating seismograph, the instrument must be designed to be launched, retrieved, and refurbished from a rolling, often wet (with salt water) ship; it must couple well to a (very!) soft or hard bottom and poorly to flowing near-bottom water. There is still much room for improvement over even the best of the existing OBS. As is the case for land instruments, probably more so, optimum design is a strong function of the observational objectives. For example, seismic noise on the ocean floor is low above about 2 Hz and often very high in the storm microseism band, three to 10 seconds. It is still uncertain how much the data are influenced by poor bottom coupling. Partially because of the high noise levels, in addition to instrumental difficulties, relatively little work has been done with long-period instruments and most of the current interest is above 1 Hz. However, interest in the long-period range is growing. At the other end of the spectrum there is interest in extending the frequency band to a few hundred (or thousand) Hz for high resolution sediment studies and acoustic studies of Navy interest.

Most existing OBS are designed for the detection of small signals, well within the linear range of bottom motion, and only such instruments will be discussed in this paper. Steinmetz et al. (1979) describe an OBS specifically designed for recording strong motion.

An excellent review paper by Whitmarsh and Lilwall (1983) provides a fairly complete general description of OBS developed and used through 1981. It includes an extensive bibliography of OBS related papers, many of which provide specification tables and schematic drawings of operational OBS. A more recent review paper by Prothero (1984) discusses the state of the art of OBS technology through 1983, based partly on a workshop held at the University of California, Santa Barbara in July 1982. Since 1970, a sequence of papers on OBS development has been published in Marine Geophysical Researches. Most of these papers are listed by Whitmarsh and Lilwall (1983). Physical characteristics of the 12 operational OBS deployed during the Lopez Island OBS intercomparison experiment (conducted in June 1978) are tabulated in Sutton et al. (1981b). Schematic drawings and additional specifications for these instruments are contained in Hawaii Institute of Geophysics Technical Report, HIG-80-4, Hawaii Institute of Geophysics, Honolulu.

In this paper I shall not attempt another comprehensive review of the field but, rather, shall limit the discussion to a brief review of the history and the current status with which I am most familiar, emphasizing research and instrument development subsequent to that reported in the Whitmarsh and Lilwall and the Prothero papers.

EARLY OBS

Ewing and Ewing (1961) describe the history and status, at that time, of OBS development. The earliest OBS were designed for small scale, active refraction experiments with both the self-contained OBS and the explosives deployed either by cable or free-fall (pop-up). In the latter case, the sensor was mechanically isolated from the flotation required for retrieval. Figure 1 is a block diagram of the acoustic telemetering OBS described by Ewing and Ewing. Data from a single vertical component 2 Hz geophone were transmitted by frequency modulation of a 12 k Hz carrier and received with a standard echo-sounder transducer. Different mechanical configurations involved either cable or free-fall deployment with no provision for retrieval of the bottom package. Both explosion and earthquake signals were well recorded with this system.

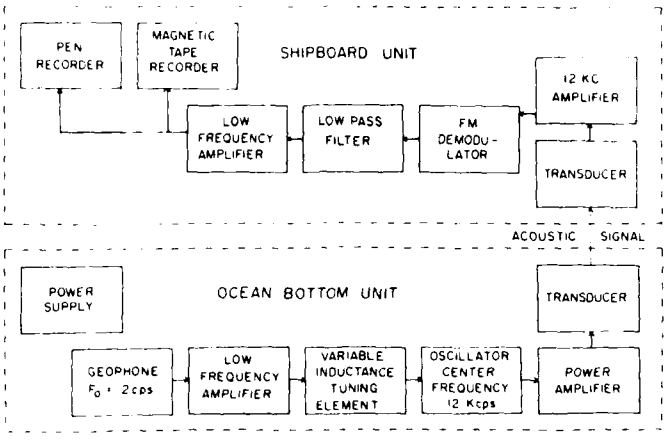

Figure 1. System block diagram of acoustic telemetering OBS (Ewing and Ewing, 1961).

Figure 2 shows the location of the Columbia (Pt. Arena) OBS, about 100 miles west of San Francisco, California in four kilometers water depth, that operated for over six years, 1966-1972 (Sutton et al. 1965 and 1969). The bottom package (Figure 3) was actually a small geophysical observatory containing: three-component long (15 second) and short (one second) period seismometers; low (crystal) and high (coil) frequency hydrophones; Vibratron tidal pressure sensor; crystal temperature sensor; and water current magnitude and direction sensors. Ultra long-period (feed-back) outputs from the long-period seismometers provided tidal gravity and tilt data. The instrument package was connected to shore at Pt. Arena, California via two-conductor deep-sea cable. Power and 30 command channels to the OBS and 18 data channels from the OBS to the shore station were transmitted through this cable. Except for the mechanical current sensor, which failed after about two months (probably from biological growth and/or silting) all instruments operated until the cable was damaged by wave activity near shore.

Data from the Columbia OBS are included in a number of reports on short- and long-range explosion experiments and studies of local seismicity and teleseisms, tides and tidal currents, and microseisms. One interesting observation is that the OBS often recorded offshore earthquakes not observed by land stations at comparable epicentral distance and the converse for on-shore earthquakes (Sutton et al., 1969).

Figure 4 illustrates the short-period signals from a local earthquake recorded by the Columbia OBS at about 250 km epicentral distance. It is of interest to note that each of the three motion components and the pressure component emphasize different aspects of the signals providing, e.g. information on direction of propagation and arrival type. The hydrophone record has the simplest character; a strong surface reflection, P_{R_1}, because of the amplification of pressure of a downgoing signal (combined with its bottom reflection) near the bottom; and lack of the shear arrival, Sn. Pn is strong on the vertical, small on H_2 (longitudinal horizontal), and missing on H_1 (transverse horizontal).

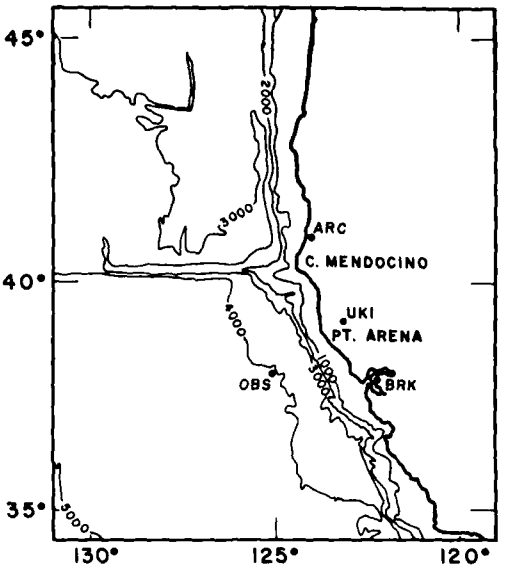

Figure 2. Location of Columbia OBS. ARC, UKI, and BRK are stations of the Berkeley (University of California) seismic network. OBS recording station was at Pt. Arena. Mendocino Escarpment trends E-W near 40°N. Depth contours in meters (Sutton et al., 1965).

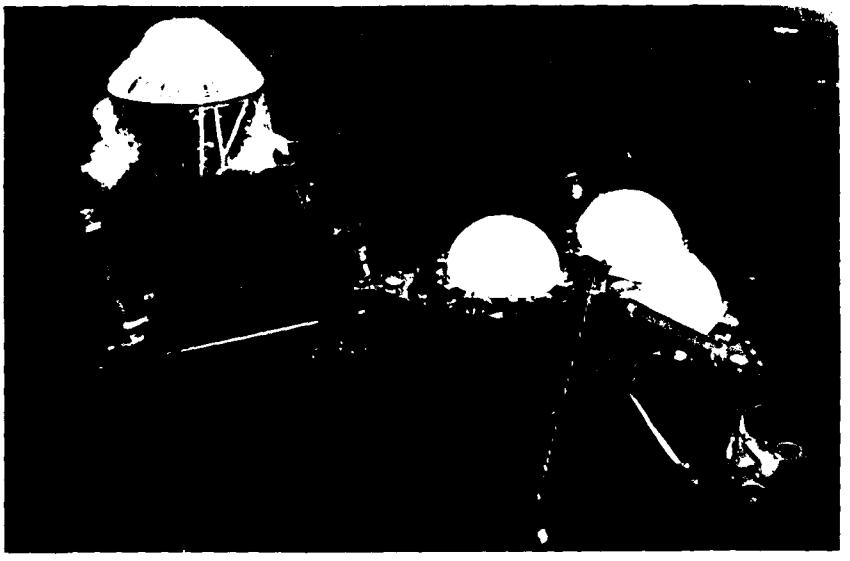

Figure 3. Columbia OBS before connection to cable. Three-component SP and LP seismometers are contained in two of white spheres. Other sensors are mounted on frame. Plastic cover on current meter was removed before lowering. Sphere diameter approximately 0.6 m (Sutton et al., 1965).

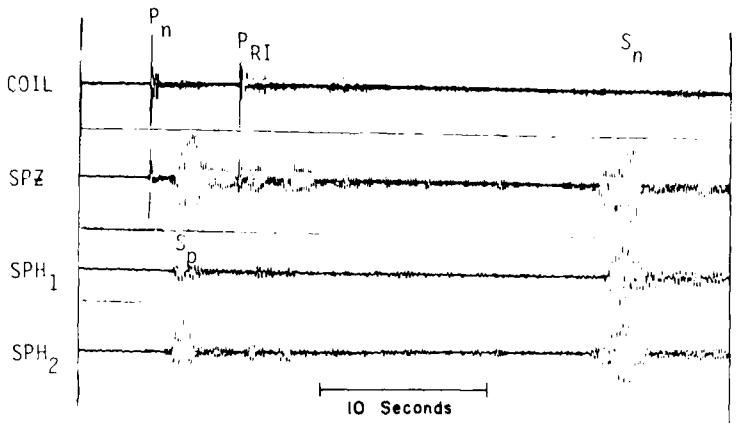

Figure 4. P and S arrivals from a local earthquake recorded by the Columbia OBS (Figures 2 and 3). Traces, from top, are: short-period hydrophone (coil); short-period vertical seismometer (SPZ); and two orthogonal short-period horizontal seismometers (SPH_1 and SPH_2). Identified arrivals are: mantle refracted P and S (Pn and Sn); surface reflected Pn (P_{RI}); and Pn converted to S at the base of the sedimentary layer (Sp) (Sutton et al., 1969).

All three seismometers record the converted wave Sp and the shear arrival Sn, which begins earlier on the vertical and longitudinal horizontal components because of partial conversion to P below the ocean bottom. The resonant character of the seismometer signals results mainly from OBS-bottom coupling resonance, to be discussed more fully later, but may be partly due to sediment velocity structure. Spectra from P, S, and T phase arrivals on a given seismometer component exhibit nearly identical resonant peaks. However, the resonant frequency is different for each component: 7, 5, and 6 Hz for Z, H_1 and H_2, respectively. This observation strongly suggests that the instruments are recording different resonant coupling modes excited by the signals (Sutton et al., 1969). Sutton et al. (1965) calculated possible resonant coupling frequencies for the Columbia OBS to be about 70 and 60 Hz for vertical and rocking motion, respectively, well above the frequency band of interest at that time. That calculation was based upon an estimated sediment shear velocity of 0.15 km/sec. More recent observations give shear velocities at the top of marine sediments an order of magnitude lower. Since the coupling frequency is proportional to the shear velocity, a velocity of 15 m/sec would produce calculated frequencies of 7 and 6 Hz, as observed in the data. It is interesting to note that most of the operational pop-up OBS tested during the Lopez Island experiment, to be discussed later, exhibited coupling frequencies between about 5 and 10 Hz and the sediment shear velocity near the bottom was measured to be 15-20 m/sec.

An array of hydrophones near Wake Island and connected by cable to the island was installed more than 25 years ago to locate nose cone impacts from intercontinental ballistic missile tests. Eleven of these phones are still operational. Six are on the ocean bottom at 5.5 km depth and make up the vertices and center of a pentagon about 40 km across; five are located at three different sites near the axis of the SOFAR channel (about 1 km depth). The combined array spans more than 300 km. Signals from eight of these hydrophones, five bottom, and three

SOFAR, have been recorded digitally by the Hawaii Institute of Geophysics on a continual basis since September 1982. The hydrophone signals are recorded through low-noise low-frequency preamplifiers and are used for seismological studies. The array is unique, both in its deep ocean location and in its great distance from other seismological stations.

McCreery et al. (1983) examine the spectral characteristics of P waves from shallow focus earthquakes and nuclear explosions and samples of ocean-bottom background noise recorded on the Wake array. Ambient noise levels on the ocean bottom near Wake are comparable to levels at the quietest continental sites for frequencies between three and 15 Hz. At lower frequencies the noise increases rapidly toward the "storm" microseism maximum near 0.2 Hz where the level is above that for continental sites.

SHALLOW WATER OBS

In a series of papers Brocher et al. (Brocher, 1983; Brocher et al., 1981 and 1983) reported on the results of a nine day OBS experiment conducted on the continental margin off Nova Scotia in June 1975. Three HIG telemetering OBS were placed in a linear array along the dip of the bottom with approximate spacing of 18 km at depths of 67, 140, and 1301 m. The lack of resonance in the recorded signals suggests that the low-profile instrument packages (7:1 length-to-diameter ratio) provided excellent coupling to the sediments for the three-component 2 Hz natural frequency geophones and avoided the coupling of the seismometers to ocean-bottom currents. The OBS were hard-wired directly to the recording ship and were anchored to the seafloor by a heavy communication cable. The broadband frequency response of both the incorporated hydrophone and the geophones together with the FM recording of the signals on (1.5 IPS) tape drives, contributed to the high quality of the recorded data. The horizontal geophones in the OBS were oriented along (horizontal longitudinal) and perpendicular (horizontal transverse) to the longest axis of the OBS package (and the cable).

Data from a variety of seismic sources were recorded during the nine day investigation. The purpose of the experiment was to study the propagation of noise produced by a drilling rig platform located approximately 18 km shoreward from the shallowest OBS. Signals and background from air gun profiling, SUS charges, shipping, biological activity, bottom current, varying weather conditions, and seismicity were investigated, in addition to the rather low level of signal observed from the drilling operations. P and S velocity structure in the subbottom was determined; S/N ratios for the hydrophones and geophones in the band one to 30 Hz were compared; and low frequency propagation along strike and up and down dip of the topography was studied. Shear velocities were obtained from analyses of both Stoneley (Scholte) and refracted shear waves.

Related studies were reported, at a previous NATO conference on bottom-interacting ocean acoustics, by Rauch (1980) and Schirmer (1980). In both of these studies tethered OBS were utilized to detect interface waves in shallow water.

BOREHOLE OBS

A number of experiments have recently been conducted using seismometers clamped in a drillhole below the ocean floor. In these experiments the drilling ship Glomar Challanger of the Deep Sea Drilling Project was used. Two papers based on data from one such installation,

located about 400 miles southeast of the central Kuril Islands are included in this volume (Duennebier et al., 1985; and Carter et al., 1985). This ocean subbottom seismograph (OSS) is emplaced 21 m below the sediment-basalt boundary at a depth of 5.85 km. The OSS includes a self-contained power and recording system that can be left on the ocean floor and retrieved and refurbished at a later time (Duennebier and Blackinton, 1983). Stephen (1981, and earlier papers) has used three-component borehole data from shots recorded on the drilling ship via direct cable connection to investigate anisotropy in the oceanic crust. Carter et al. (1984) compared data from an OSS emplaced in soft sediment at a depth below bottom of 194 m with that from an HIG ISOBS (described later in the section on Isolated Sensor OBS). The OSS and OBS exhibited remarkably similar S/N characteristics. Absolute noise levels were similar above 10 Hz but below 10 Hz the OSS was quieter by three to eight dB.

Another borehole seismograph, the Marine Seismic System (MSS), is similar in design concept but more elegant that the OSS (Ballard et al., 1984). Shearer and Orcutt (1985) detected and analyzed anisotropy within the oceanic lithosphere using MSS and OBS data collected during the NGENDEI seismic experiment in early 1983, about 500 miles east of the Kermadec Trench in the southwest Pacific.

Absolute noise levels for the OSS and MSS, when clamped in competent rock beneath the sediment, are significantly lower than for OBS on adjacent ocean-bottom, especially for the horizontal components of motion. S/N also appears to be higher for most transient signals.

THE ROSE EXPERIMENT

The Rivera Ocean Seismic Experiment (ROSE) was a large combined sea and land seismic program utilizing both explosive sources and earthquakes to study the structure and evolution of a mid-ocean ridge, a major oceanic fracture zone and the transition region between ocean and continent (Ewing and Meyer, 1982). Because permission was not received to conduct the experiment in Mexican territorial waters as originally planned, the marine portion was relocated from the Rivera Fracture Zone to the East Pacific Rise south of the Orozco Fracture Zone. The two month field program (January-March 1979) involved many cooperating research groups and a large number of OBS. Preliminary results are given in a series of papers in the same number of Journal of Geophysical Research as the Ewing and Meyer overview paper (Project ROSE Special Issue, J. Geophys. Res., 87, B10, 1982). These and subsequent papers (e.g. Bratt and Purdy, 1984; Bratt and Solomon, 1984; Trehu and Purdy, 1984) provide a great deal of information on the P and S crustal velocity structure of the Orozco Fracture Zone and East Pacific Rise in that vicinity and on the local seismicity. In addition to the scientific results, ROSE has provided useful lessons for possible future large cooperative efforts and modifications in instrument design concerning such disparate items as data archiving and distribution; optimum joint location of instruments and ships; instrument turn-around time and reliability; timed versus acoustic recall; and OBS data capacity and timed versus triggered versus continuous recording.

A paper by Rowlett and Forsyth (1984), which discusses microearthquakes observed at the intersection of the Vema Fracture Zone and the Mid-Atlantic Ridge, provides an interesting comparison with similar studies from ROSE on the more rapidly spreading East Pacific Rise.

ISOLATED SENSOR OBS

In most of the OBS used today, the sensors, electronics, recorders, flotation, and ballast are contained in one rigid package. This configuration requires a relatively large mass and large vertical cross section in the water that can result in poor coupling to the bottom, and increased noise level from response to water flow (Duennebier et al., 1981). The use of an isolated sensor can minimize these problems. In addition, separation between the sensors and the main OBS package reduces the effect of possible vibrations from the data recorder. An isolated sensor OBS (ISOBS) developed at Hawaii Institute of Geophysics (Byrne et al., 1983) is shown in Figure 5. The cylinder containing the geophones is held rigidly to the main package during free-fall and is released after arrival at the bottom by the solution of a magnesium retaining pin. Direct comparison between signals recorded by a single package OBS of earlier HIG design and the ISOBS, deployed near each other in deep water, clearly demonstrated the advantages of the isolated sensor configuration. Additionally, at the Lopez Island tests, the two OBS with separated sensors (ISOBS and another supplied by MIT) exhibited bottom coupling characteristics superior to those of the single package OBS.

Although data suggest that the ISOBS is a considerable step toward improving the fidelity of OBS recording, an improved prototype isolated sensor has since been developed at HIG (Figure 6) known as the "Opihi" (after an Hawaiian limpet that adheres to underwater surfaces). The "Opihi package attempts to optimize the three principal design parameters found to affect sensor coupling to the ocean bottom (Sutton et al., 1981a,b). The parameters are: (1) a plate with a relatively large surface area for low bearing pressure, (2) nearly neutral density, allowing the package to "float" in the sediments and (3) a buried package, for greater coupling to solid material and less exposure to ocean bottom currents.

The "Opihi" package deals with these three parameters by mounting the ISOBS geophone pressure case on a plate framework. This plate is then inserted into a soft mesh bag filled with a loose matrix of polyvinylchloride pellets (PVC) or pea gravel. This method distributes the weight of the pressure case over a wide area, making it about neutral density in soft sediments (total package specific gravity of about 1.4). The loose matrix also simulates a buried sensor and should appear as a small bump on soft sediments. The package has the additional advantage that it can conform to bottom contours and couple well on hard or soft bottoms. The low profile of the package makes it relatively insensitive to ocean bottom currents.

In essence, this sensor package should have good coupling and low noise generation on any type of surface. Initial testing of the "Opihi" sensor package design has shown that it improves coupling over the previous ISOBS sensor package. At this writing, the "Opihi" has not been implemented in an operational OBS.

CURRENT AND DESIRED OBS OPERATIONAL SPECIFICATIONS

In 1984, Rondout Associates, Incorporated conducted a survey of OBS developers and users. Following is an abbreviated summary derived from the 34 responses received indicating required and desired specifications (with this author's comments indicated by GHS):

Major Interests: most investigators are interested in Velocity Structure and Local Seismicity. Fewer are interested in Focal

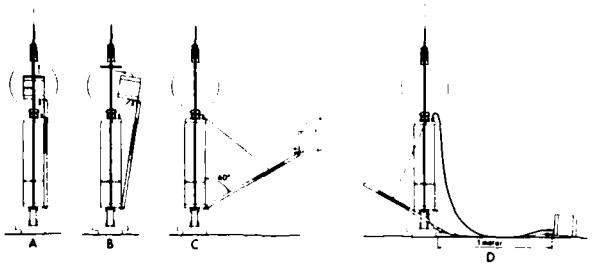

Figure 5. Isolated sensor OBS geophone release scheme. Separation is approximately one meter (Byrne et al., 1983).

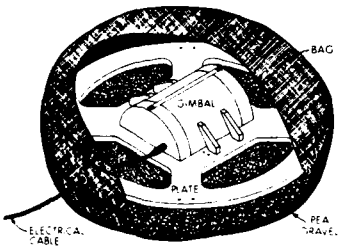

Figure 6. "Opihi" isolated sensor package. Scale length is 0.5 meters (Byrne et al., 1983).

Mechanism and Exploration/Prospecting. There is less general interest in Teleseismic Studies and Engineering applications.

Maximum Depth: most want capability to Normal Ocean (6000m) depth; a few need capability to work in Trenches (12,000m); fewer still require or desire Intermediate (2000m) or Continental Shelf (500m) maximum depth. The interest in shallower depth coincides with Engineering and Strong Motion interests.

Frequency Range: the median required frequency range is two to 30 Hz; a maximum overall range of 0.01 to 100 Hz. The median desired range is one to 100 Hz and the maximum overall range is DC-4 kHz! Wider band instruments emphasize either LP or HF, typically three decades.

Components Required: most require or desire three-component seismometers and a hydrophone. Anything less is generally a compromise for data storage or other reasons. (Each of the four components provides unique information. However, since the hydrophone generally produces relatively clear and simple records with good S/N, relatively undisturbed by poor bottom coupling and current noise, it is sometimes preferred for exploration and acoustic work.-GHS)

Recording: everybody requires or desires digital recording. Some stick to analog recording (for good reason!-GHS) because of the great advantages of continuous recording in the marine environment; limitations of digital data quantity; problems with triggering on noise, and not-triggering on weak signals; and logistical problems with timed recording.

Recording Mode: most investigators require or desire a

Microprocessor Controlled system and prefer the Triggered Mode to the Timed Mode. (Peal and Kirk, 1983, describe a versatile microprocessor-controlled OBS data logging system. This subject is also covered by Prothero, 1984.-GHS) A significant number require (or currently have) Continuous Recording.

Recording Medium: the majority currently use Cassette Recorders; some use or would prefer Reel-to-Reel or Cartridge recorders. Most of those using digital recording would desire greater capacity than their existing system. (The recorder is a major problem area. In addition to problems with storage capacity, it is the major power drain, is one of the least reliable components, and can be an important source of vibration noise. The OBS community would welcome a real breakthrough in this area.-GHS)

Dynamic Range: the median required dynamic range is 72 dB; the responses range from 26 dB (analog) to 96 dB without gain ranging and 130 dB with gain ranging. The median desired dynamic range is 120 dB; the responses range from 60 to 80 dB and 40 dB plus AGC to 150 dB, 16 bit floating point.

Deployment Time: the median required Deployment Time is 30 days with a total range from one day to one year. The median desired deployment time is six months with a range of one day to "semi-permanent". The short times are from groups principally interested in Shelf and Intermediate Depth Engineering studies and/or Exploration/Prospecting; the long times coincide with interest in Teleseismic and Long Period work.

Recording Time: the answers to this item are given in terms of continuous recording times (analog), the number of short event time windows; and/or the total number of megabytes (mB) data storage capacity. The median values listed are approximate. The median required Recording Capacity is about 20 mB, digital; or 20 to 30 days, analog. The required values range from 20 minutes (5 mB) to 90 mB, digital; and four days to two months, analog. The median desired Recording Capacity is about 100 mB digital and three to six months, analog. The values range from about 40 mB to ∞, digital, and one month to one year, analog. (As noted before, under Recording Medium, this is an area that needs improvement.-GHS)

Acceptable Clock Drift: (the important thing is uncorrectable drift. Linear drift can be corrected.-GHS) The acceptable uncertainty depends upon the experimental objectives. Total uncertainty of +/- 0.1 second or less is required for most earthquake work. Short-period array studies and high resolution sediment studies require near 1 msec accuracy. Total clock stability of one part in 10^9 is desirable.

Maximum Weight: the median required Maximum Weight is 150 kg with values ranging from 45 kg. to $<$ 450 kg. The median desired maximum weight is $\leq$ 90 kg. with values ranging from 10 kg to 300 kg.. A few investigators who work from large ships are relatively unconcerned about weight. Workers with more limited ship capabilities and personnel and/or who utilize a larger number of instruments are concerned to keep weight and handling difficulties to a minimum.

Release: everyone prefers an acoustic release, generally with a timed release backup. (Use of acoustic telemetry for diagnostics is useful. An associated transponder used for precision navigation is invaluable for certain experiments.-GHS)

Bottom Coupling: (I have viewed this as a major problem area for a number of years.-GHS) All require good coupling to soft bottoms and most to rocky bottoms. Fewer are concerned with High Currents. (Refer to further discussion below under Packaging Configurations.-GHS)

Azimuthal Orientation: most require or desire an independent measurement of azimuth. The median preferred accuracy is +/- 5° with a range of values from 0.5 to 10°.

Packaging Configuration: a majority of the respondents require or desire either Separated Sensors or Low Profile or both; two, indicate (strong) preference for a single package; one suggests an adaptable system depending upon bottom conditions. (The Lopez Island experiment indicated that the coupling performance of isolated sensor package OBS is better than single package instruments, although some of the latter performed almost as well. The isolated sensor instruments produced records comparable to the three special "standard" instruments used at Lopez Island (Sutton et al., 1981b).

Use of a well-designed separated sensor package generally should improve the bottom coupling and isolation from current induced and tape recorder noise. It should also be a more flexible design permitting various sensor packages and a common support and recording package. The requirement of including flotation and retrieval aids on a single package instrument makes optimum coupling design difficult. However, generally an isolated sensor design is more complex and, therefore, less reliable.-GHS)

Retrieval: everyone wants a Flasher and Radio (although the Radio antenna can be a serious source of current-induced noise-GHS). Several require or desire an acoustic pinger and/or transponder to aid in retrieval.

Maximum Unit Cost: the majority listed $10-20,000; a significant number prefer <$10,000; or will accept $20-40,000; and a few will go to >$40,000. Generally, the higher values coincide with more stringent OBS requirements.

General Evaluation of Current OBS Designs-(GHS)

Major problem areas or areas where improvements are needed include bottom-coupling (signal distortion) and noise; data storage; system reliability, especially over long deployment times; ease of handling during launch and retrieval; and ease of shipbound checkout before and after deployment. Each of the OBS with which I have personal familiarity, principally those used in the Lopez and ROSE experiments, has some strong and weak points. The external configurations of many of the OBS were modified subsequent to Lopez to improve coupling characteristics.

The trade offs between analog and digital have been discussed earlier. Most investigators prefer the digital route. The limited dynamic range of analog recording can be alleviated by gain ranging on background noise, multiple gain channels, and temporary digital storage and subsequent gain range before analog recording. Much digital data have been lost by poor trigger algorithms and other problems.

Reliability has been a serious problem with some systems, both from lost data and from lost instruments. The acceptable loss rate depends upon the cost and uniqueness of the data and the instrument package. Some groups have experienced very low rates; and others 10% or more. Occasionally, losses come in batches. Details of each component and the system as a whole must be considered carefully. External sensors (seismometers and hydrophones) require pressure tight electrical leadthroughs; cables to isolated sensors can become caught on the anchor or bottom rocks. Release mechanisms can fail; glass instrument and flotation spheres can fail after repeated use.

Some systems are difficult to launch and retrieve without damage; some of the larger instruments require special handling gear. Some systems require extensive, time-consuming pre-launch checkout, limiting the

number of instruments that can be deployed for a given experiment. The conflicting technical requirements or desires of the OBS community for low-power and low-instrument volume, versus high data storage, high dynamic range and high clock stability are pushing the state of the art.

SIGNAL DISTORTION AND NOISE IN OBS

A badly designed OBS can be subject to severe signal distortion because of poor coupling to the soft ocean bottom and suffer from high levels of noise caused by near-bottom water currents shaking the instrument frame. Most existing operational OBS exhibit some amount of these undesirable characteristics. The seismic frequency response of an OBS frame of a given mechanical configuration coupled to sediment of a given shear velocity (V_S) and density can be predicted using relationships that have been tested experimentally using in situ mechanical transients. These same relationships can be used to establish guidelines for designing instruments with improved coupling response. Seismic signals couple to an OBS both through the area(s) of contact with the sediment and directly through the contact with the water. Assuming that the desired response is to faithfully follow the motion of the sediment surface, direct coupling to the water for horizontal-translation and rocking modes of motion should be minimized. The OBS will follow the sediment motion for frequencies lower than the natural frequencies of the modes of coupling motion. Thus, it is generally desired to have these coupling frequencies (f_c) as high as possible. For a given OBS configuration, there is an optimum effective radius for the area of coupling to the sediment that will produce the highest predictable coupling frequency. The optimum radius is proportional to the cube root of the instrument mass. Using these optimum radii, the coupling frequency decreases as the cube root of the mass, i.e. smaller instruments will have higher (more favorable) coupling frequencies.

Recognizing the importance of the OBS-bottom coupling problem, the Lopez Island OBS experiment was conducted in Shoal Bay, Lopez Island in June 1978, as a preliminary to ROSE, in order to compare the responses of the operational OBS, which have quite varied mechanical configurations, when coupled to the earth through soft sediments comparable to those of the ocean floor, and to determine their susceptibility to noise induced by near-bottom currents (Sutton et al., 1981b). (More recently, a similar experiment involving a different set of OBS was conducted in France; I am not aware of published results.) The maximum current measured during the test was 6 cm/sec and no significant correlation was found with noise on the OBS during the experiment.

Signals recorded on OBS geophones are often narrow band and prolonged (Figure 4). Whether these features are natural in origin or caused by the presence of the OBS was a major question to be answered by the test. Some data indicated that the presence of the OBS on the soft sediments could severely distort the motion of the ground; however, the extent of this problem for OBS of different configurations was unknown. The complications present on many geophone records are not observed on ocean bottom hydrophones, thus the question: do geophone data add any useful information that cannot be obtained from hydrophones?

Some data had indicated that near-bottom currents can increase noise levels on OBS enough to make them unusable during high-current periods; therefore, we wanted to test as many systems as possible for susceptibility to ocean current noise.

In addition to 12 operational OBS supplied by 10 different research organizations, three sets of three-component (T_o=1s) seismometers and a hydrophone were included to provide standards for comparison: a "spike standard" was pushed firmly into the bottom; a "plate standard" with a smooth, hemispherical superstructure on a large, flat, circular plate was placed on the sediments; and a "neutral density standards" with a roughly spherical shape was floated within the uppermost sediment. The instruments were placed within a few meters of each other, and four current meters were installed around the array to monitor water circulation in the bay.

Data were obtained from each sensor by hard wiring analog signals to land where they were recorded by a digital system. Seismic records were obtained from mechanical transient tests, airgun shots and blasting caps, and samples of background noise. Mechanical transient tests were conducted to provide some quantitative estimate of the coupling function between the ocean bottom and the OBS package, including possible cross coupling between horizontal and vertical motions. The procedure is analogous to the classical weight lift test for earthquake seismographs, although because of buoyancy the response of the seismic system to the mechanical transient test is not the same as that to a seismic input (Sutton et al., 1981a).

An Hawaii Institute of Geophysics Technical Report (HIG-80-4) contains a large number of records from each recorded sensor. The technical report also shows the designs of all instruments. All the data of this experiment are on digital tapes and may be requested from the ROSE data archive at Hawaii Institute of Geophysics. A catalog of the data appears in the technical report.

Subsequent to the Lopez Island experiment, a number of papers on bottom coupling have improved our understanding of the problem and provided guidelines for better OBS design (Sutton et al., 1981 a and b; Zelikovitz and Prothero, 1981; Lewis and Tuthill, 1981; Trehu, 1985; Garmany, 1984; Sutton et al., 1985; and Sutton and Duennebier, 1985).

Table I lists parameters that must be considered and Table II summarizes possible problems of signal distortion and noise related to OBS-bottom coupling. A schematic diagram of the dynamic coupling between an OBS and a soft bottom for vertical motion is shown in Figure 7. In general, the spring "constant", K, is not equal to the static value; both K and the damping "constant", D, are functions of frequency. The inertial effect of the water, Mw*, and sediment, Ms*, involved in the differential motion between the OBS and its surroundings may also be considered to be frequency dependent (or alternatively included in the variation in K). The M*, K, and D are also shape dependent.

The case for horizontal input is similar to that for vertical motion, with the added complications that: there can be two independent inputs in each orthogonal direction, one through the water and one through the sediment; and cross-coupled rocking motion can contribute a major portion of the output from the horizontal seismometers (and from the vertical, if it is located far from the center of rotation). The response of a horizontal geophone to a rocking mode tilt, θ, is equivalent to a horizontal acceleration, $\ddot{y}_t=g\theta$, so that the total apparent input is $\ddot{y}+\ddot{y}_t$.

The response of a rigid sphere in a fluid to a seismic signal in the fluid of wavelength large compared to the sphere diameter is U/V-3/(2(Mi/Mw)+1) where U and V are the motion of the sphere and the incident wave in the fluid, respectively, and Mi and Mw are the mass of

TABLE I
OBS-BOTTOM COUPLING PARAMETERS

A. OBS
1. Mass
2. Moments of Inertia
3. Structural Rigidity
4. Symmetry
5. Shape/Smoothness
6. Cross-Section to Water
7. Cross-Section to Sediment
8. Density
9. Bearing Area
10. Bearing Pressure
11. Burial

B. SEDIMENT/ROCK
1. Density
2. Shear Velocity
3. Anelasticity
4. Heterogeneity
5. Permeability

C. WATER
1. Density
2. Viscosity
3. Sound Velocity

D. INTERFACES/STRUCTURE
1. Water-Sediment Interface Roughness
2. Sediment-Rock Interface Roughness
3. Velocity-Depth Dependence

TABLE II
OBS-BOTTOM COUPLING PROBLEMS

SIGNAL DISTORTION

OBS on Sediment
-Vertical Output from Vertical Signal
-Horizontal Output from Horizontal Signal
-Vertical Output from Horizontal Signal
-Horizontal Output from Vertical Signal

OBS on Rock
-Rattling
-Large Tilt
-"Floating" Footpad

Direct OBS-Water Coupling
-Discontinuous Horizontal Signal Across Water/Sediment Boundary
-Inertial Effect (Most OBS have Large Internal Vertical Gradient in Density)

Lateral Heterogeneity of Bottom

Tilts on Horizontals from Ultra-Low Phase Velocity Signals

NOISE

OBS on Sediment
-Amplification of Microseisms at Bottom Interface
-Signal Induced "Noise" from Irregular Boundary
-Water/Sediment
-Sediment/Layer 2

Direct OBS-Water Coupling
-Current Induced Noise

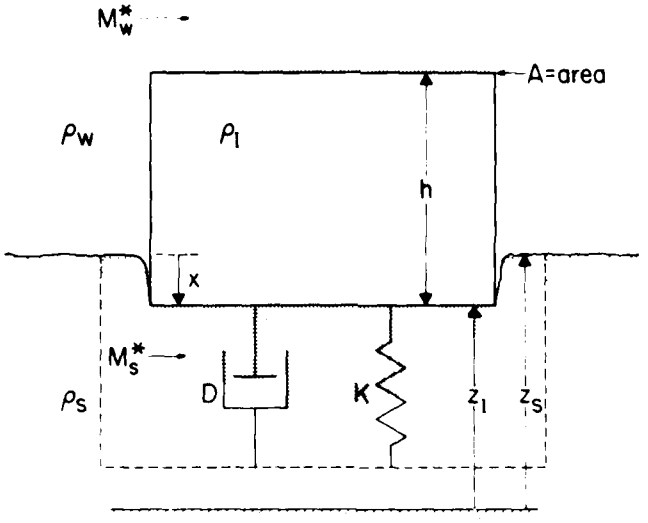

Figure 7. Schematic of OBS coupling to ocean bottom for vertical motion. The dashed line is assumed to move with the ocean floor adjacent to the OBS (Sutton et al., 1981a).

the sphere and the displaced water, respectively. Similar relationships hold for bodies of other shapes. Since current OBS designs generally include most of the body of the instrument within the water, direct seismic coupling between water and OBS is certain and in many cases could be more important than coupling through the bottom sediments. From the equation, we see that amplification can approach a factor of three for very low sphere densities and that attenuation occurs for densities greater than water. As expected, when Mi=Mw, U=V. Most OBS contain low-density flotation for retrieval in their upper portion and more dense disposable anchoring material near the bottom-coupling interface. This density gradient, in addition to producing torques from equal amplitude horizontal inputs, will modify the response from waves having different horizontal amplitudes in the water and in the sediment (e.g. horizontally propagating compressional waves or horizontally polarized shear waves). The vertical component is less complicated since signal amplitude is continuous across the water-sediment boundary and most OBS have appreciable symmetry about a vertical axis. However, lateral variations within the bottom under the OBS could affect this component, also.

A simple calculation indicates the possibility of significant noise resulting from response to tilts produced by bottom currents. Consider a spherical OBS with cross section $1 m^2$, centered in the water 1/2 m above two circular footpads of radius 0.2 m that are separated by 1 m in the direction of the current, resting on sediment with shear velocity 20 m/sec and density 1 g/cm^3. The vertical displacement of the footpads (one up, one down) from a bottom current of 5 cm/sec is about 10 μm. This is roughly 10^3 larger than the vertical signal from a teleseismic P

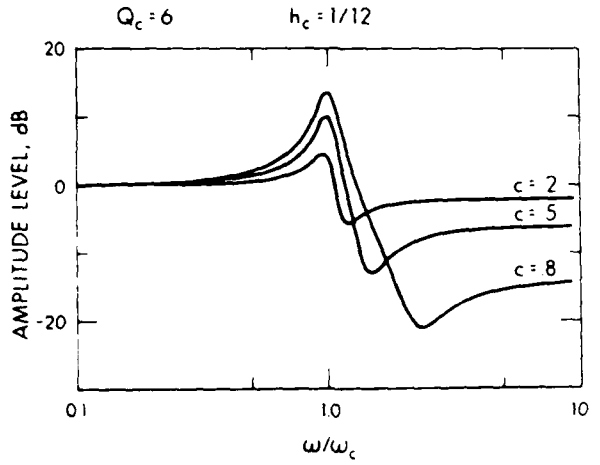

Figure 8. OBS package seismic response for underdamped coupling (Sutton et al., 1981a).

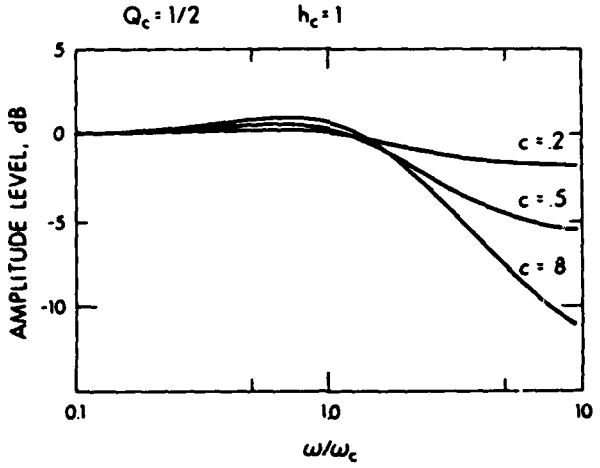

Figure 9. OBS package seismic response for critically damped coupling (Sutton et al., 1981a).

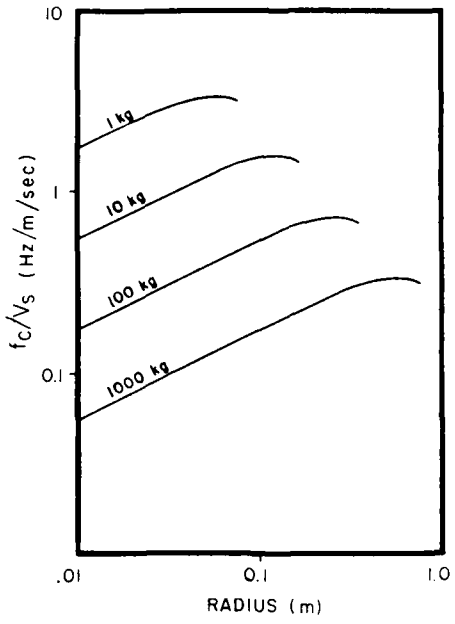

Figure 10. OBS resonant coupling frequency, fc, as a function of radius of bottom-coupling area and instrument mass. Normalized by shear velocity of bottom, V_S. Curves terminate at limit of second-order theory (Sutton and Duennebier, 1985).

wave. The horizontal acceleration associated with the tilt ($\ddot{y}=g\theta$) is equivalent to a horizontal amplitude of 200 μm at 6 second period. This value is about 20 times larger than the horizontal signal from average "storm" microseismic. Small perturbations of bottom currents around such large mean values should produce significant noise on most operational OBS.

Figures 8 and 9 show the amplitude response of an OBS to a seismic input, assuming frequency independent coefficients, for two values of damping and three values of the coupling coefficient c. It can be seen that the OBS will faithfully follow the input for frequencies well below the coupling resonance, ωc, but that serious distortion can occur near resonance and significant attenuation can occur at higher frequencies. The coupling coefficient, c, depends upon the OBS density (as indicated earlier for a sphere in water). c=0 is neutral density; and gives perfect coupling independent of ωc. These response curves are reliable to frequencies somewhat above ωc, but there is some question regarding their precision at higher frequencies (Trehu, 1985; Sutton and Duennebier, 1985).

The relationship from second-order theory between coupling frequency and bearing radius (assuming a circular bearing area) for OBS of different mass is shown in Figure 10. For a given mass, the coupling frequency increases with radius to a maximum value near the limit of validity of the theory. The damping also increases with radius and is near critical at the maximum of these curves. Thus, it appears that the radius of the maximum is also the optimum design radius for a given OBS.

Note, also, that the larger the OBS the more difficult it is to obtain a high coupling frequency.

From the foregoing, Sutton and Duennebier (1985) arrived at the following desired parameters for OBS design: (1) minimum mass, (2) optimum radius in contact with ocean floor for a given instrument mass, shape and sediment density, (3) density approximately that of the sediment, (4) sensors near the center of mass/vertical symmetry, and (5) small cross section within the water. The "Opihi" (Figure 6) satisfies these requirements quite well.

Garmany (1984) presents a generalized procedure for recovering true ocean bottom particle motion using only the output signals from a three-component OBS that have been distorted by coupling and/or the local bottom conditions. Sutton et al. (1985) point out some problems with Garmany's analysis. A modified version of Garmany's method might be used to improve the quality of existing OBS data, but I believe it is not a substitute for good OBS design.

ACKNOWLEDGEMENTS

This research was supported, in part, by contracts with Office of Naval Research, Air Force Office of Scientific Research, and Defense Advanced Research Projects Agency of the United States Government.

REFERENCES

Ballard, J.A., C.C. Mulchahy, R.L. Wallerstedt, and E.L. Kiser, 1984, The Borehole Seismic Experiment in Hole 395A: Engineering and Installation, in R.D. Hyndman, M.H. Salisbury, et al., Init. Repts. DSDP, 78, Washington (U.S. Govt. Printing Office), 743-758.

Bratt, S.R. and G.M. Purdy, 1984, Structure and Variability of Oceanic Crust and Flanks of the East Pacific Rise Between 11° and 13°N, J. Geophys. Res., 89, 6111-6125.

Bratt, S.R. and S.C. Solomon, 1984, Compressional and Shear Wave Structure of the East Pacific Rise at 11° 20'N: Constraints from Three-Component Ocean Bottom Seismometer Data, J. Geophys. Res., 89, 6095-6110.

Brocher, T.M., 1983, Shallow Crustal Structure of the Continental Margin off Nova Scotia, Can. J. Earth. Sci., 20, 1657-1672.

Brocher, T.M., J.F. Gettrust, G.H. Sutton, and L.N. Frazer, 1981, Comparison of the S/N Ratio of Low Frequency Hydrophones and Geophones as a Function of Ocean Depth, Bull. Seis. Soc. Am., 71, 1649-1659.

Brocher, T.M., B.T. Iwataki, and D.A. Lindwall, 1983, Experimental Studies of Low-Frequency Water-Borne and Sediment-Borne Acoustic Wave Propagation on a Continental Shelf, J. Acoust. Soc. Am., 74, 960-972.

Byrne, D.A., G.H. Sutton, J.G. Blackinton, and F.K. Duennebier, 1983, Isolated Sensor Ocean Bottom Seismometer, Marine Geophys. Res., 5, 437-449.

Carter, J.A., F.K. Duennebier, and D.M. Hussong, 1984, A Comparison Between a Downhole Seismometer and a Seismometer on the Ocean Floor, Bull. Seis. Soc. Am., 74, 763-772.

Carter, J.A., G.H. Sutton, A. Suteau-Henson, and F.K. Duennebier, 1985, Analysis of Ocean Subbottom Seismograph (OSS) Data, this volume.

Duennebier, F.K. and G. Blackinton, 1983, The Ocean Subbottom Seismometer, in Geophys. Exploration at Sea, R. Geyer, Ed., CRC Press, Boca Raton, Florida, 317-332.

Duennebier, F.K., G. Blackinton, and G.H. Sutton, 1981, Current-Generated Noise Recorded on Ocean Bottom Seismometers, Marine Geophys. Res., 5, 109-115.

Duennebier, F.K., R. Cessaro, and P. Anderson, 1985, Deep-Ocean Bore-Hole Seismo-Acoustic Results from the North-West Pacific Ocean, this volume.

Ewing, J. and M. Ewing, 1961, A Telemetering Ocean-Bottom Seismograph, J. Geophys. Res., 66, 3863-3878.

Ewing, J.I. and R.P. Meyer, 1982, Rivera Ocean Seismic Experiment (ROSE) *Overview*, J. Geophys. Res., 87, 8345-8358.

Garmany, J.D., 1984, The Recovery of True Particle Motion from Three-Component *Ocean Bottom* Seismometer Data, J. Geophys. Res., 89, 9245-9252.

Lewis, B.T.R. and J.D. Tuthill, 1981, *Instrumental* Waveform Distortion on Ocean Bottom Seismometers, Marine Geophys. Res., 5, 79-86.

McCreery, C.S., D.A. Walker, and G.H. Sutton, 1983, Spectra of Nuclear Explosions, Earthquakes, and Noise from Wake Island Bottom Hydrophones, Geophys. Res. Let., 10, 59-62.

Peal, K.R. and R.E. Kirk, 1983, An Event Recording Ocean Bottom Seismograph, 1983 IEEE Proc. Third Symp. Oceanographic Data Systems, IEEE Comp. Soc. Press, Silver Springs, Maryland, 114-118.

Prothero, W.A., Jr., 1984, Ocean Bottom Seismometer Technology, EOS, 113-116.

Rauch, D., 1980, Experimental and Theoretical Studies of Seismic Interface Waves in Coastal Waters, in Bottom-Interacting Acoustics, W.A. Kuperman and F.G. Jensen, Ed., Plenum Press, New York, 307-327.

Rowlett, H. and D.W. Forsyth, 1984, Recent Faulting and Microearthquakes at the Intersection of the Vema Fracture Zone and the Mid-Atlantic Ridge, J. Geophys. Res., 89, 6079-6094.

Schirmer, F., 1980, Experimental Determination of Properties of the Scholte Wave in the Bottom of the North Sea, in Bottom-*Interacting* Acoustics, W.A. Kuperman and F.G. Jensen, Ed., *Plenum Press*, New York, 285-298.

Shearer, P. and J. Orcutt, 1985, Anisotropy in the Oceanic Lithosphere--*Theory and Observations* from the NGENDEI Seismic Refraction Experiment in the Southwest Pacific, Geophys. J. R. Astr. Soc., 80, 493-526.

Steinmetz, R.L., P.L. Donoho, J.D. Murff, and G.V. Latham, 1979, Soil Coupling of a Strong Motion, Ocean Bottom Seismometer, Proc. Offshore Tech. Conf. Houston, 2235-2249.

Stephan, R., 1981, Seismic Anisotropy Observed in Upper Oceanic Crust, Geophys. Res. Let., 8, 865-868.

Sutton, G.H. and F.K. Duennebier, 1985, Optimum Design of Ocean Bottom Seismometers, Marine Geophys. Res., in press.

Sutton, G.H., F.K. Duennebier, and G.J. Fryer, 1985, *Comment* on "The Recovery of True Particle Motion from Three-Component Ocean Bottom Seismometer Data" by Jan D. Garmany, J. Geophys. Res., in press.

Sutton, G.H., F.K. Duennebier, and B. Iwataki, 1981a, Coupling of Ocean Bottom Seismometers to Soft Bottom, Marine Geophys. Res., 5, 35-51.

Sutton, G.H., F.K. Duennebier, B. Iwataki, J.D. Tuthill, B.T.R. Lewis, and J. Ewing, 1981b, An Overview and General Results of the Lopez Island OBS Experiment, Marine Geophys. Res., 5, 3-34.

Sutton, G.H., G. McDonald, D.D. Prentiss, and S.N. Thanos, 1965, Ocean-Bottom Seismic Observations, Proc. IEEE, 53, 1909-1921.

Sutton, G.H., M.E. Odegard, N. Mark, and N.J. Letourneau, 1969, Research in Seismology Related to the Columbia Ocean-Bottom Seismo-

graph, Hawaii Institute of Geophysics Final Report to AFCKL/ARPA, HIG-70-12, 66p.

Trehu, A.M., 1985, Coupling of Ocean Bottom Seismometers to Sediment: Results of Tests with the U.S. Geological Survey Ocean Bottom Seismometer, Bull. Seis. Soc. Am., 75, 271-289.

Trehu, A.M. and G.M. Purdy, 1984, Crustal Structure in the Orozco Transform Zone, J. Geophys. Res., 89, 1834-1842.

Whitmarsh, R.B. and R.C. Lilwall, 1983, Ocean-Bottom Seismographs, in Structure and Development of the Greenland-Scotland Ridge, Bott, Saxov, Talwani, and Thiede, Ed., Plenum Press, New York, 257-286.

Zelikovitz, S.J. and W. Prothero, 1981, Vertical Response of an Ocean Bottom Seismometer: Analysis of the Lopez Island Vertical Transient Tests, Marine Geophys. Res., 5, 53-67.

JOURNAL OF GEOPHYSICAL RESEARCH, VOL. 90, NO. B13, PAGES 11,567–11,568, NOVEMBER 10, 1985

Comment on "The Recovery of True Particle Motion From Three-Component Ocean Bottom Seismometer Data" by Jan D. Garmany

GEORGE H. SUTTON

Rondout Associates, Incorporated, Stone Ridge, New York

FRED K. DUENNEBIER AND GERARD J. FRYER

Hawaii Institute of Geophysics, University of Hawaii, Honolulu

Garmany [1984] presents a procedure for recovering the true ocean bottom particle motion using the output signals from a three-component ocean bottom seismometer (OBS). In the abstract he states, "The most significant implication of this work is that accurate ground motion can be recovered from almost any three-component OBS." This is a worthy objective, since it is well known that much OBS data are degraded because of poor coupling through soft bottom sediments and water. The paper provides an interesting generalized approach that might be used to improve OBS data if some serious errors and omissions contained in the paper are properly corrected and considered.

Garmany [1984] assumes that the OBS has three inputs and three outputs and that the OBS site system is an all-pole minimum delay filter. He indicates that these two assumptions are required in order for the procedures outlined in the paper to be valid. However, in general, an OBS has five independent rectilinear seismic inputs: one vertical input and four horizontal inputs, two from the bottom sediment and two from direct coupling to the near-bottom water, which moves differently from the bottom for various seismic wave types. Additionally, the transfer function for a seismic input contains one or two zeros as well as poles. We now consider further each of Garmany's two assumptions.

The response of a rigid sphere in a fluid to a seismic signal in the fluid of a wavelength which is large compared to the sphere diameter is $U - V = 3/(2M_t/M_w) + 1)$, where U and V are the motion of the sphere and the incident wave in the fluid, respectively, and M_t and M_w are the mass of the sphere and the displaced water, respectively [*Batchelor*, 1967]. Similar relationships hold for bodies of other shapes. Since current OBS designs generally include most of the body of the instrument within the water, direct seismic coupling between water and the OBS is certain and in many cases could be more important than coupling through the bottom sediments. From the equation we see that amplification can approach a factor of 3 for very low sphere densities and that attenuation occurs for densities greater than water. As expected, when $M_t = M_w$, $U = V$. Most OBS's contain low-density flotation for retrieval in their upper portion and more dense disposable anchoring material near the bottom-coupling interface. This density gradient, in addition to producing torques from equal amplitude horizontal inputs, will modify the response from waves having different horizontal amplitudes in the water and in the sediment (for example, horizontally propagating compressional waves or horizontally polarized shear waves). The vertical component is less complicated, since signal amplitude is continuous across the water-sediment boundary and most OBS's have appreciable symmetry about a vertical axis. However, as pointed out by Garmany, lateral variations within the bottom under the OBS could affect this component, also.

The response of an OBS to a vertical seismic input was given by *Sutton et al.* [1981a] and *Zelikoritz and Prothero* [1981]. Following the presentation of Sutton et al.:

$$\frac{I}{Z_v} = (1 - C)\left[s^2 + \frac{2h_v\omega_v}{(1 - C)}s + \frac{\omega_v^2}{(1 - C)}\right]/(s^2 + 2h_v\omega_v s + \omega_v^2)$$

where

- I amplitude of OBS in inertial space, that is, input to geophones;
- Z_v amplitude of incident wave;
- C $(M_t - M_w - M_s)/M_t^*$;
- h_v damping coefficient of bottom coupling;
- ω_v resonant frequency of bottom coupling;
- s transform variable ($s = j\omega$ for sinusoidal input);
- M_t instrument mass;
- M_w mass of displaced water;
- M_s mass of displaced sediment (usually negligible);
- M_t^* inertial mass of instrument plus water and sediment that move with it.

Although derived for vertical motion, when interpreted correctly the equation can be used for other motion components as well. The transfer function contains one or two zeros, depending upon the coupling coefficient C: two zeros if $C \neq 1$ and one zero if $C = 1$. The case $C = 1$ implies that $M_w = M_s = 0$ and $M_t^* = M_t$; that is, no displaced water or sediment and no additional inertia from water and or sediment. This form of the equation has been used by earlier workers to describe the motion of a geophone on a compliant surface [e.g., *Safar*, 1978]. The zero in the transfer function in this case is related to the radiation damping from the differential motion between the geophone and the soil. The transfer function is also consistent with the relation given above for the motion of a sphere in a fluid. In the absence of a bottom-related spring constant, $\omega_v = 0$, and when $C = 0$ (that is, neutral buoyancy, $M_t = M_w$), then $I = Z_v(U - V)$. Additionally, when $C = -2$, then $I = 3Z_v(U - V = 3)$. As mentioned earlier, this is the limiting condition when $M_t = M_s = 0$ and $M_t^* = M_w$. M_w is the appropriate "virtual" mass to be added to the inertial mass of a sphere moving in a fluid [*Batchelor*, 1967].

Garmany [1984] refers to *Sutton et al.* [1981a, b] and to *Zelikoritz and Prothero* [1981] and states that (in these

Paper number 4B5373
0148-0227/85/004B-5373$02.00

papers) data from the Lopez Island OBS experiment "... indicate that the restoring forces due to buoyancy are 2 or more orders of magnitude less than the effective spring constant of the sediments." This is correct and means that the modification to the coupling frequency ω_c by gravitational restoring forces on the OBS's tested at Lopez is minor, but it does not mean that all effects of buoyancy are negligible. Table V of *Sutton et al.* [1981*b*] lists values of C_{max}, which is the coupling coefficient defined above with M_i substituted for M_i^* in the denominator (that is, not including the inertial contribution of the water and/or sediment). The computed values of C_{max} for operational OBS's listed in Table V range from 0.11 to 0.53; actual values for C are still smaller, and the effect of buoyancy is hardly negligible. For neutral buoyancy, $C = 0$, the transfer function predicts perfect coupling, $I = Z_s$, independent of the coupling frequency and damping.

Garmany [1984] states further

> The fundamental difference between the present work and previous work on OBS coupling is that the author believes that the motion of the earth is communicated to the OBS by the effective spring constant of the sediments and not the far less significant forces of buoyancy.

He suggests that proper interpretation of the position variables used by *Sutton et al.* [1981*a*] would indicate that buoyancy had negligible effect on coupling response.

The validity of the transfer function given above is difficult to verify with field experiments. However, *Sutton and Duennebier* [1985] reproduced its general predictions in model experiments on a shaking table with the package both in air and submerged in water and for both vertical and horizontal inputs and outputs. A transfer function of the same form can also be used for a rocking mode response to a horizontal input [*Hsieh*, 1962].

Garmany [1984] tested his procedure using OBS data and was able to reduce spectral peaks presumably caused by coupling. Unfortunately, the signals resulting from this procedure cannot represent "true particle motion" as they are obtained using an incorrect parameterization. Since Garmany assumes that the coupling acts as an all-pole filter, he appropriately models the discrete time series as an autoregression (AR). However, as we have shown, the correct response contains both poles and zeros, so the correct parameteric time series model is not an autoregression but an autoregressive moving average (ARMA). It is well known that if the moving average (MA) part of an ARMA process is of finite order, then modeling the process as an autoregression will require an infinite order [*Box and Jenkins*, 1970, chapter 3). Hence Garmany's treatment, fitting three-channel AR models of order 4 or 8 only (that is, 12 or 24 poles), can never be expected to perform well. A dramatic improvement in performance could be expected if an AMRA model were fit to the data rather than a pure AR model. If our theory is correct (and the shake table results seem to confirm it), then an ARMA (2,2) (a second-order autoregressive, second-order moving average) is the correct model to fit.

We should warn that any parametric model fitting, be it AR, MA, or ARMA, is designed to explain correlations in the time series. If such a parametric model is used as a basis for filtering, the output will be optimally uncorrelated (white) for the model chosen. Hence such procedures have the effect of reducing all spectral peaks and will reduce those related to geology as well as those caused by coupling. Garmany acknowledges this possibility.

A filter obtained by fitting a parametric time series model to OBS data may prove valuable in reducing the effects of coupling, but it cannot be a substitute for better OBS design. We agree with Garmany that the value of proper engineering of OBS's is still considerable and that any design which reduces the in situ resonances of a seismometer will be a significant advance. It is clear that in OBS design we must strive for high-coupling frequency, near-critical damping, low direct water coupling, and low-coupling coefficient C [*Sutton and Duennebier*, 1985].

REFERENCES

Batchelor, G. K., *An Introduction to Fluid Dynamics*, 615 pp., Cambridge University Press, New York, 1967.

Box, G. E. P., and G. M. Jenkins, *Time Series Analysis Forecasting and Control*, Holden-Day, Oakland, Calif., 1970.

Garmany, J. D., The recovery of true particle motion from three-component ocean bottom seismometer data, *J. Geophys. Res.*, *89*, 9245–9252, 1984.

Hsieh, T. K., Foundation vibrations, *Proc. Inst. Civ. Eng.*, *22*, 211–226, 1962.

Safar, M. H., On the minimization of the distortion caused by the geophone ground coupling, *Geophys. Prospect.*, *26*, 538–549, 1978.

Sutton, G. H., and F. K. Duennebier, Optimum design of ocean bottom seismometers, *Mar. Geophys. Res.*, in press, 1985.

Sutton, G. H., F. K. Duennebier, and B. Iwatake, Coupling of ocean bottom seismometers to soft bottom, *Mar. Geophys. Res.*, *5*, 35–51, *1981a*.

Sutton, G. H., F. K. Duennebier, B. Iwatake, J. Tuthill, B. Lewis, and J. Ewing, An overview and general results of the Lopez Island OBS experiment, *Mar. Geophys. Res.*, *5*, 3–34, 1981*b*.

Zelikovitz, S. J., and W. Prothero, The vertical response of an ocean bottom seismometer: Analysis of the Lopez Island vertical transient tests, *Mar. Geophys. Res.*, *5*, 53–67, 1981.

F. K. Duennebier and G. J. Fryer, Hawaii Institute of Geophysics, University of Hawaii, 2525 Correa Road, Honolulu, HI 96822.

G. H. Sutton, Rondout Associates, Incorporated, P. O. Box 224, Stone Ridge, NY 12484.

(Received November 30, 1984;
revised January 19, 1985;
accepted February 20, 1985.)

UNCLASSIFIED

SECURITY CLASSIFICATION OF THIS PAGE

ADA173890

REPORT DOCUMENTATION PAGE

1a. REPORT SECURITY CLASSIFICATION: Unclassified	1b. RESTRICTIVE MARKINGS: N.A.
2a. SECURITY CLASSIFICATION AUTHORITY: ---	3. DISTRIBUTION/AVAILABILITY OF REPORT: Unlimited
2b. DECLASSIFICATION/DOWNGRADING SCHEDULE: ---	
4. PERFORMING ORGANIZATION REPORT NUMBER(S): ---	5. MONITORING ORGANIZATION REPORT NUMBER(S): N.A.
6a. NAME OF PERFORMING ORGANIZATION: Rondout Associates, Inc. / 6b. OFFICE SYMBOL (If applicable): ---	7a. NAME OF MONITORING ORGANIZATION: Same as sponsor
6c. ADDRESS (City, State and ZIP Code): P.O. Box 224, Stone Ridge, NY 12484	7b. ADDRESS (City, State and ZIP Code): ---
8a. NAME OF FUNDING/SPONSORING ORGANIZATION: Office of Naval Research / 8b. OFFICE SYMBOL (If applicable): 420	9. PROCUREMENT INSTRUMENT IDENTIFICATION NUMBER: N00014-83-C-0009
8c. ADDRESS (City, State and ZIP Code): 800 N. Qunicy St., Arlington, VA 22217	10. SOURCE OF FUNDING NOS. — PROGRAM ELEMENT NO.: / PROJECT NO.: N.A. / TASK NO.: / WORK UNIT NO.:
11. TITLE (Include Security Classification): Fidelity, Coherence and Noise of Ocean Bottom Seismographs and Hydrophones	
12. PERSONAL AUTHOR(S): G. H. Sutton	
13a. TYPE OF REPORT: Final / 13b. TIME COVERED: FROM 82Nov01 TO 85Sept30	14. DATE OF REPORT (Yr., Mo., Day): 1986 October 31 / 15. PAGE COUNT: 68
16. SUPPLEMENTARY NOTATION: ---	
17. COSATI CODES — FIELD: / GROUP: / SUB. GR.:	18. SUBJECT TERMS (Continue on reverse if necessary and identify by block number): Ocean bottom seismographs, design, bottom and water coupling, signal distortion.

19. ABSTRACT (Continue on reverse if necessary and identify by block number)

In this research we investigated the mechanical coupling between an OBS and the ocean floor for both vertical and horizontal motion and the hydrodynamic coupling between an OBS and the near bottom water, both at seismic amplitudes and frequencies and at those associated with near bottom currents. Criteria for optimum design of OBS were developed based upon both theoretical and experimental information. Current status of OBS design was summarized and evaluated.

20. DISTRIBUTION/AVAILABILITY OF ABSTRACT: UNCLASSIFIED/UNLIMITED ☒ SAME AS RPT. ☐ DTIC USERS ☐	21. ABSTRACT SECURITY CLASSIFICATION: Unclassified
22a. NAME OF RESPONSIBLE INDIVIDUAL: Paul W. Pomeroy	22b. TELEPHONE NUMBER (Include Area Code): (914) 687-9150 / 22c. OFFICE SYMBOL: ---

DD FORM 1473, 83 APR — EDITION OF 1 JAN 73 IS OBSOLETE.

Unclassified

SECURITY CLASSIFICATION OF THIS PAGE

END

DATE
FILMED

12-86

DTIC